TERATOLOGY 49:497–517 (1994)

Methanol-Induced Neural Tube Defects in Mice: Pathogenesis During Neurulation

BRAD BOLON, FRANK WELSCH, AND KEVIN T. MORGAN

Department of Experimental Pathology and Toxicology, Chemical Industry Institute of Toxicology, Research Triangle Park, North Carolina 27709 (B.B., F.W., K.T.M.); Integrated Toxicology Program, Duke University, Durham, North Carolina 27710 (B.B.)

ABSTRACT A spectrum of cephalic neural tube defects was observed in near-term (gestation day [GD] 17) mouse fetuses following maternal inhalation of methanol at a high concentration (15,000 ppm) for 6 hr/day during neurulation (GD 7–9). Dysraphism, chiefly exencephaly, occurred in 15% of fetuses, usually in association with reduction or absence of multiple bones in the craniofacial skeleton and ocular anomalies (prematurely open eyelids, cataracts, retinal folds). Measurements of cerebrocortical width in grossly normal, methanol-exposed fetuses revealed significant semiquantitative differences in the thicknesses of the frontal cortex and its constituent layers (neuroepithelium, intermediate cortex/subventricular plate, and cortical layer 1) as well as apparent increases in subventricular plate cellularity relative to controls. Subsequently, the early morphogenesis of these neural changes was investigated in neurulating mouse embryos to define tissue-specific patterns of methanol-induced damage that lead to cephalic axial dysraphism. Following daily 6-hr maternal inhalations of 15,000 ppm methanol during GD 7–8, the cephalic neural fold margins were swollen, blunted, and poorly elevated on GD 8.5 and 9 relative to controls. Histopathology of exposed GD 8.5 embryos revealed microcephaly in association with reductions in the cell density and mitotic index of at least 47% in the cranial mesoderm. The mitotic index in the embryonic neuroepithelium was also reduced by 55%, and groups of neural crest cells were displaced to the neural folds dorsal to the foregut (relative to the more ventral location in the facial regions of control embryos). When examined on GD 9.5 and 10.5, maternal methanol exposure (15,000 ppm for 6 hr/day) during GD 7–9 resulted in stunting, delayed rotation, and microcephaly in over 90% of the affected embryos. Persistent patency of the anterior neuropore and prosencephalic hypoplasia were seen in >40% and up to 90% of embryos, respectively. Shallow optic vesicles, stunted branchial arches, scoliosis, and hydropericardium were also observed. Many 10.5-day-old embryos were edematous. Occult dysraphism, recognized grossly by abnormally narrow cephalic conformation and histopathologically by the absence of mesoderm in the mesencephalon, was present in at least 21% of methanol-exposed embryos on GD 9.5 and 10.5. Nile blue vital dye staining of methanol-exposed embryos revealed no difference in dye accumulation between control and treated embryos on GD 8.5, 9.0, or 9.5. There were no apparent dysmorphogenic effects in control embryos at any stage of development. These data suggest 1) that exposure to a high concentration of methanol injures multiple stem cell populations in the neurulating mouse embryo and 2) that significant neural pathology may remain in older conceptuses even in the absence of gross lesions.

Cephalic axial dysraphism (or neural tube defects) is currently among the most common lethal birth defects that occur in humans (Campbell et al., '86). Anecdotal evidence suggests that there may be an increased incidence of such lesions in human populations clustered near sources of chemical contamination to the environment (U.S. News, '91). Neural tube defects are also among the more common malformations observed in rats and mice following maternal exposure to a variety of chemicals (Shepard, '86; Szabo, '89), including high concentrations of methanol vapors (Nelson et al., '85; Bolon et al., '93; Rogers et al., '93). The proposed heavier reliance on methanol-based automobile fuels to curb air pollution in the urban United States may result in elevated atmospheric concentrations of this chemical (Posner, '75). While adult humans are more sensitive than rodents to the acute neuroocular toxic

Received January 7, 1994; accepted March 11, 1994.

Address reprint requests to Dr. Brad Bolon, Pathology Associates, Inc., 15 Worman's Mill Court, Suite I, Frederick, MD 21701.

Presented in part at the 44th Annual Meeting of the American College of Veterinary Pathologists, San Antonio, Texas, December 5–10, 1993.

effects of methanol (Roe, '82; Kavet and Nauss, '90), the relative vulnerabilities of rodent and human conceptuses are unknown. Thus, one issue of concern is that the human conceptus may be placed at increased risk for the development of brain (and other) terata by maternal contact with higher environmental levels of methanol.

Two assumptions are required when extrapolating data from methanol teratogenicity studies in rodents to estimate the potential for inducing developmental toxicity in human conceptuses. One is that the toxic moieties will be the same in these species. This premise is supported by studies showing that adult rodents with a reduced capacity to detoxify formate (the putative methanol-derived neurotoxicant) develop functional and structural changes that are comparable to those observed in adult human patients with methanol toxicity (Makar and Tephly, '77; Eells, '91), while normal rodents are resistant because they metabolize formate efficiently (Roe, '82). Methanol and formate accumulate in tissues of neurulating mouse embryos following maternal inhalation of methanol at a teratogenic concentration (Bolon and Welsch, unpublished data). Thus, mouse conceptuses are exposed to these toxicant(s) at the phase of embryogenesis during which dysraphic defects are induced (Bolon et al., '93). A second supposition is that target cell populations will be similar in rodent and human embryos. That this may be true is suggested by the observation that events defining the process of neural tube development and closure are homologous in both species (Campbell et al., '86; Marin-Padilla, '91; Jacobson, '92).

The next steps are to elucidate the nature of the dysmorphogenic process (e.g., failed elevation of neural folds vs. failed fusion after elevation) and to identify groups of potential target cells that participate in the formation of the brain and cranium and are injured by exposure to methanol. Insight into the possible sites of methanol-induced damage may be inferred from developmental toxicity data obtained with ethanol (Streissguth et al., '80). Prior studies with this well-known human teratogen using neurulating mouse and avian conceptuses suggest the existence of multiple populations of sensitive cells, including the neuroepithelium (Kotch and Sulik, '92a,b), neural crest (Kotch and Sulik, '92a), and paraxial mesoderm (Sulik et al., '81; Sanders et al., '87). It is not known whether these findings are applicable to methanol-induced defects in neural tube closure. Classical pathological techniques provide an effective means by which these questions may be investigated.

The present studies were designed to identify the scope of methanol-induced cephalic terata in fetal mice and to determine potential target sites in neurulating embryos that could account for their presence. Following maternal methanol inhalation at a high, teratogenic concentration during the time of neural tube development and closure, localization of dysraphic malformations to the brain and craniofacial bones of near-term fetuses suggested that one or more of the embryonic stem cells from which these tissues originate (e.g., neuroepithelium, neural crest, paraxial mesoderm) were sensitive to methanol. Neural tube defects, microcephaly, and craniofacial malformations in methanol-exposed embryos correlated well with findings in fetuses. Lesions in embryos were associated with consistent, severe reductions in cell number and mitotic index in the paraxial mesoderm, the mitotic index of the neuroepithelium, and the apparent area of the neural crest. However, neither histopathologic examination nor vital dye staining revealed primary sites of damage in these three embryonic tissues. Finally, the present studies showed that organization of the cerebral cortex was altered in grossly normal, methanol-exposed fetuses, indicating that significant neural pathology may remain in older conceptuses in the absence of gross lesions. These data should significantly enhance current efforts to assess health hazards posed to the human conceptus by maternal exposure to methanol.

MATERIALS AND METHODS

Animals

Young adult Crl:CD-1 ICR BR (CD-1) mice (Charles River Laboratories, Raleigh, NC) were housed in polycarbonate cages (1 male or 5 females/cage) containing paper bedding (ALPHA-dri™, Shepherd Specialty Papers, Kalamazoo, MI). Mice received NIH-07 pelleted diet (Zeigler Brothers, Gardner, PA) and filter-purified tap water ad libitum, except during the 6-hr treatment period when food was removed. Cages were kept in biologically clean rooms with HEPA-filtered air and a 12-hr light/dark cycle. Temperature was maintained at 21–23°C and relative humidity at 45–55%. After 14 days in quarantine, nulliparous females (25–35 g) were paired 1:1 in the home cages of the males for the last 2 hr of the dark cycle. Females with copulation plugs were immediately weighed and identified using a metal ear tag, and this day was designated as gestation day (GD) 0.

Experimental design

Dams were exposed to methanol (0 or 15,000 ppm for 6 hr/day) from GD 7–9, which encompasses the period of murine neurulation (Nishimura and Shiota, '77) and the time of greatest vulnerability to methanol-induced neural tube defects (Bolon et al., '93). Near-term (GD 17) fetuses were examined to identify neural and craniofacial terata. Embryos were examined either during (GD 8.5, 9) or immediately after (GD 9.5, 10.5) neural tube closure to evaluate methanol-induced disruptions in cephalic morphogenesis that could account for the spectrum of fetal lesions. These time points were selected because chemically induced lesions generally oc-

cur in neurulating embryos by 6–12 hr following toxicant exposure (Sulik et al., '88; Kotch and Sulik, '92a).

Test material and administration

Daily inhalation exposures to either methanol (high performance liquid chromatographic [HPLC] grade, J.T. Baker, Inc., Phillipsburg, NJ) or HEPA-filtered air were conducted in 1 m^3 stainless-steel and glass, Hinners type inhalation chambers (Harford Metal Products, Inc., Aberdeen, MD). The test atmosphere was produced using a wick generator (Decker et al., '82) with fluid-metering pump and nitrogen as a carrier gas. The chamber methanol concentration was sampled every 20 min during the 6-hr treatment period using infrared detection (Miran 1A, Foxboro Co., South Norwalk, CT); an average level (± standard deviation [SD]) of 15,060 ± 250 ppm was achieved within 15 min of initiating exposure to reach a target concentration of 15,000 ppm. Chamber levels for different days of exposure varied by less than 3.3%. Dams were housed individually in hanging stainless-steel mesh cages during the exposure and then transferred to filter-capped polycarbonate cages (4 mice/cage).

Maternal observations

Toxicity was assessed in the dams by daily clinical examinations both before and following exposures and by determination of terminal maternal body weights.

Fetal pathology

Dams were killed with carbon dioxide on GD 17 (n = 25 controls, 20 treated). Near-term fetuses were removed from the uterus, blotted, weighed, fixed by immersion in Bouin's solution for 96 hr, and then transferred to 70% ethanol. Heads of selected control (n = 2–3/litter, chosen at random) and most methanol-exposed fetuses with gross dysraphic malformations were detached and cut transversely into 5 blocks using free hand cross sections (Fig. 1) guided by external landmarks (adapted from Barrow and Taylor, '69; Kaufman, '92). A few heads were divided along the mid-sagittal plane to facilitate the comparison of normal and abnormal relationships between neural and skeletal elements, particularly relative positions and proportions (Marin-Padilla, '91). Head blocks were dehydrated in graded alcohols, embedded in paraffin, and cut at 6 μm. Sections were stained with hematoxylin and eosin. In addition to qualitative morphological comparisons, the thickness of various layers in the left frontal cortices (Fig. 2) of overtly normal fetuses was quantified using an ocular reticule (Cambridge Instruments, Buffalo, NY) calibrated with a stage micrometer (Nikon). The intermediate cortex and subventricular plate were measured together because the border between them was irregular and often indistinct. Finally, 10 control and 8 exencephalic fetuses examined on GD 17 were double-stained and cleared to evaluate the extent and degree of ossification in the craniofacial

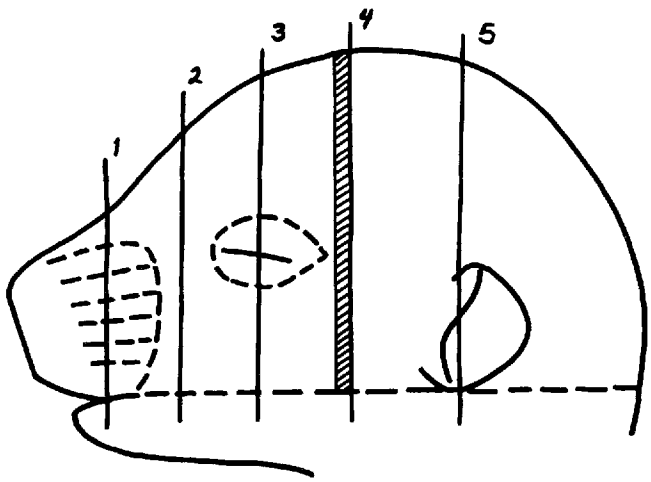

Fig. 1. Profile of a fetal mouse head demonstrating external landmarks by which free hand transverse cross sections (frontal planes 1–5) were oriented to obtain reproducible sections for histopathological examination. Cerebrocortical measurements were gathered from sections taken through the hatched region.

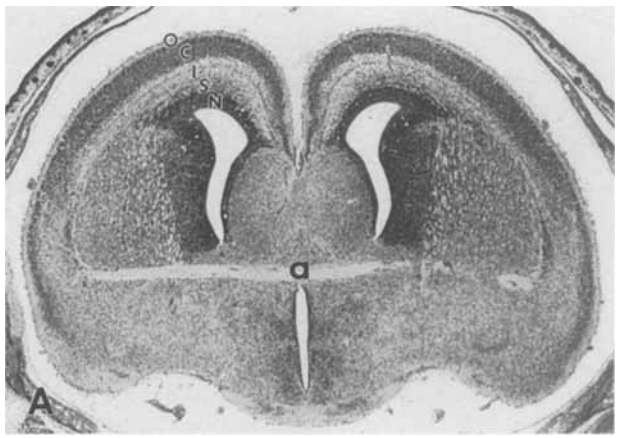

Fig. 2. Transverse section through the forebrain of a GD 17 mouse fetus (taken through the hatched region in Fig. 1) showing the site at which cortical thickness was measured. N, cortical neuroepithelium; S, subventricular plate; I, intermediate zone; C, cortical plate; O, cortical layer 1; a, anterior commissure. Hematoxylin & eosin, ×5.

skeleton (Kimmel and Trammell, '81). Briefly, unfixed fetuses were eviscerated, placed in hot water (about 75°C) for 1 min, skinned, and then immersed for 96 hr in 70% ethanol containing 0.001% alcian blue, 0.002% alizarin red S, and 14% glacial acetic acid. Tissues were cleared by sequential transferral at 12-hr intervals through 2% potassium hydroxide (KOH), 1% KOH, and a 1:1 mixture of 1% KOH with glycerin. Cleared fetuses were stored in pure glycerin.

Embryo pathology

Gross pathology and measurements. Dams were killed with carbon dioxide on GD 8.5, 9.0, 9.5, or 10.5

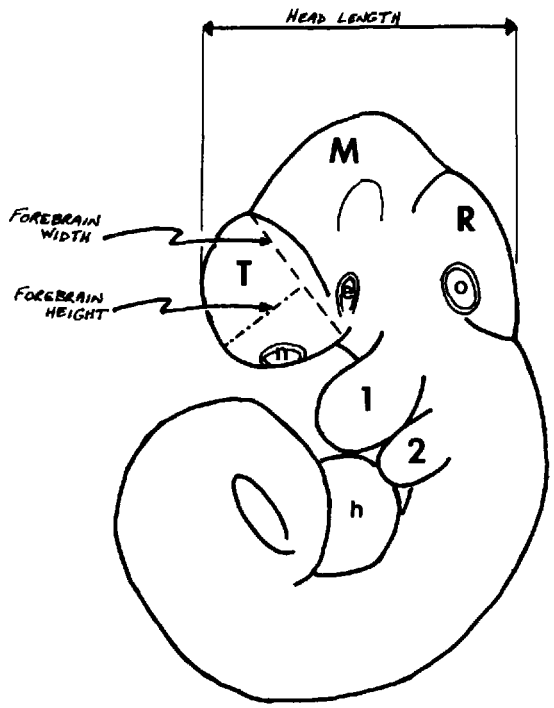

Fig. 3. Schematic drawing of embryonic measurements applied to a control embryo (GD 9.5 embryo, about 20 somites). T, telencephalon; M, mesencephalon; R, rhombencephalon; e, optic vesicle; h, heart; n, nasal placode; o, otic pit; 1 and 2, first and second branchial arches.

(n = 3–5/time for controls, 4–9/time for treated). The uterus was removed and placed in warm Tyrode's buffer; all manipulations were done at 37°C. Embryos (n = at least 30 controls and 55 treated per time) were removed from the uterus and embryonic membranes, examined grossly under a stereomicroscope, and evaluated using a standard developmental scale (Brown, '90). Lengths of the body, head, and prosencephalon as well as the prosencephalic height (Fig. 3) were measured on embryos with closed anterior neuropores at GD 9.0, 9.5, and 10.5 as previously described (Turner et al., '90) using an ocular reticule (Graticules LTD, Tonbridge, England) calibrated with a stage micrometer (Nikon).

Histopathology and morphometric analysis. Most embryos were then fixed in Bouin's solution for 96 hr and washed in 70% ethanol. Fixed embryos (n ≥ 5/group for all GD) were selected at random, dehydrated in graded alcohols, and embedded in paraffin. Serial 6-μm-thick sections were stained with hematoxylin and eosin prior to microscopic examination. For GD 8.5 embryos (n = 8 controls, 27 treated), the cell density (total number of cells; Coelho and Klein, '90) and mitotix index (ratio of dividing cells to the total cell number; Cole and Trasler, '80) were measured in neuroepithelium and cranial mesoderm using a different reticule (Cambridge Instruments). For both measurements, cells in a 25 μm^2 area were counted from both right and left sides of each region in three adjacent sections taken through the cephalic neural folds. The six counts were averaged to obtain the value for each embryo.

Scanning electron microscopy. Twenty GD 9.5 embryos (n = 5 controls, 15 treated) were immediately processed for ultrastructural evaluation by immersion fixation in ice-cold 2.5% glutaraldehyde in 0.1 M phosphate (Sorenson's) buffer. After at least 5 days at 4°C, fixed embryos were washed for 5 min and then stored overnight in Sorenson's buffer, post-fixed in 1% osmium tetroxide in Sorenson's buffer, and then washed again in Sorenson's buffer for 30 min. Embryos were dehydrated at 22°C in graded alcohols (30 min each for 50%, 70%, 95%, and 100%) and then transferred overnight to hexamethyldisilizane (Polysciences, Inc., Warrington, PA) at 22°C. Embryos were mounted on chucks using colloidal silver paste (Ted Pella, Inc., Tustin, CA) and sputter-coated under vacuum using a gold-palladium electrode. Coated embryos were examined immediately using a scanning electron microscope (Model JSM-840A, JEOL, Peabody, MA).

Vital dye staining. Some embryos (n = 4–6/litter) were stained for 30 min in Nile blue sulfate (Sigma Chemical Co., St. Louis, MO) mixed 1:50,000 in phosphate buffered saline (pH 7.6) (Sulik et al., '88) on GD 8.5, 9.0, and 9.5. At least 25 control and 30 treated embryos were examined for each time except for the GD 9.0 control group, in which only 17 were processed. Stained conceptuses were evaluated using a stereomicroscope.

Statistical analysis

A one-way analysis of variance (ANOVA) and Scheffe's F-test were used to assess maternal and fetal weights as well as differences in cerebrocortical layer thicknesses of fetal brains, using the individual animal as the experimental unit. Terminal weights for 3/20 GD17 dams were excluded from the maternal weight analysis because their litters had been entirely resorbed. The percentages of dead and malformed embryos per litter were analyzed using the Mann-Whitney U-test, in which the litter was considered the experimental unit. Differences in cell density and mitotic index in embryonic tissues also were analyzed with the Mann-Whitney U-test, using the embryo as the experimental unit. Significance was determined for all results at $P \leq 0.05$.

RESULTS

Maternal toxicity

Inhalation of methanol at 15,000 ppm on GD 7–9 induced signs of neurologic distress in up to 15% of dams each day, including ataxia, circling, tilted heads, or depressed motor activity. One mouse was removed from the study on GD 7 due to the severity of clinical signs; its uterus contained one hemorrhagic embryo.

TABLE 1. Body weights[1] of near-term mouse fetuses following maternal inhalation of methanol

Treatment	Grouping for analysis	No. of litters	Average body weights (g)
Control	All litters	25	0.92 ± 0.05
Methanol[2]	All litters	17[3]	0.82 ± 0.02*
	Litters with neural defects	11	0.79 ± 0.03*
	Litters without neural defects	6	0.87 ± 0.02

[1]Values are mean ± SE.
[2]Exposure to 15,000 ppm for 6 hr/day during GD 7–9.
[3]Analysis excludes 3 litters in which all fetuses were resorbed.
*$P \leq 0.05$, significant difference from age-matched controls by ANOVA and Scheffe's F-test.

All other affected dams had recovered within 12 hr after exposure had ended. An association between the occurrence of maternal toxicity and the presence of fetal toxicity and malformations was not apparent. As described previously (Bolon et al., '93), near-term (GD 17) maternal body weights of dams that had inhaled methanol were significantly reduced relative to those of age-matched controls. In contrast, terminal body weights of control and methanol-exposed dams were comparable at all earlier times during gestation (data not shown).

Fetal pathology

Growth. Near-term (GD 17) body weights were lower in methanol-exposed fetuses than in controls. The extent of this reduction averaged 14% for litters in which gross neural terata were observed and 6% in litters without brain malformations (Table 1). This deficit was significantly different from controls only for those litters in which neural terata were observed.

Neural defects. A spectrum of gross neural defects was seen in mouse fetuses exposed as embryos to methanol. As reported previously (Bolon et al., '93), cephalic neural tube defects were present in about 15% of near-term fetuses whose dams had inhaled 15,000 ppm of methanol on GD 7–9. Exencephaly (X, Fig. 4) was the most common form of neural dysraphism (91% of affected fetuses; Bolon et al., '93). In anencephalic fetuses (3%), the absence of craniodorsal brain regions (e.g., cerebrum, cerebellum) left a small ridge of brainstem exposed in the caudal quadrant of the open cranial vault (A, Fig. 4). Encephaloceles (3%) presented as red, midline nodules located on the forehead behind the eyes (E, Fig. 4). Holoprosencephaly (3%) was characterized by the presence of a single, asymmetric cerebral

Fig. 4. Spectrum of cephalic axial dysraphic defects in near-term (GD 17) mouse fetuses induced by maternal inhalation of methanol (15,000 ppm, 6 hr/day) during GD 7–9. C, normal; E, encephalocele; X, exencephaly, with or without facial clefting; A, anencephaly; H, holoprosencephaly (with anophthalmia).

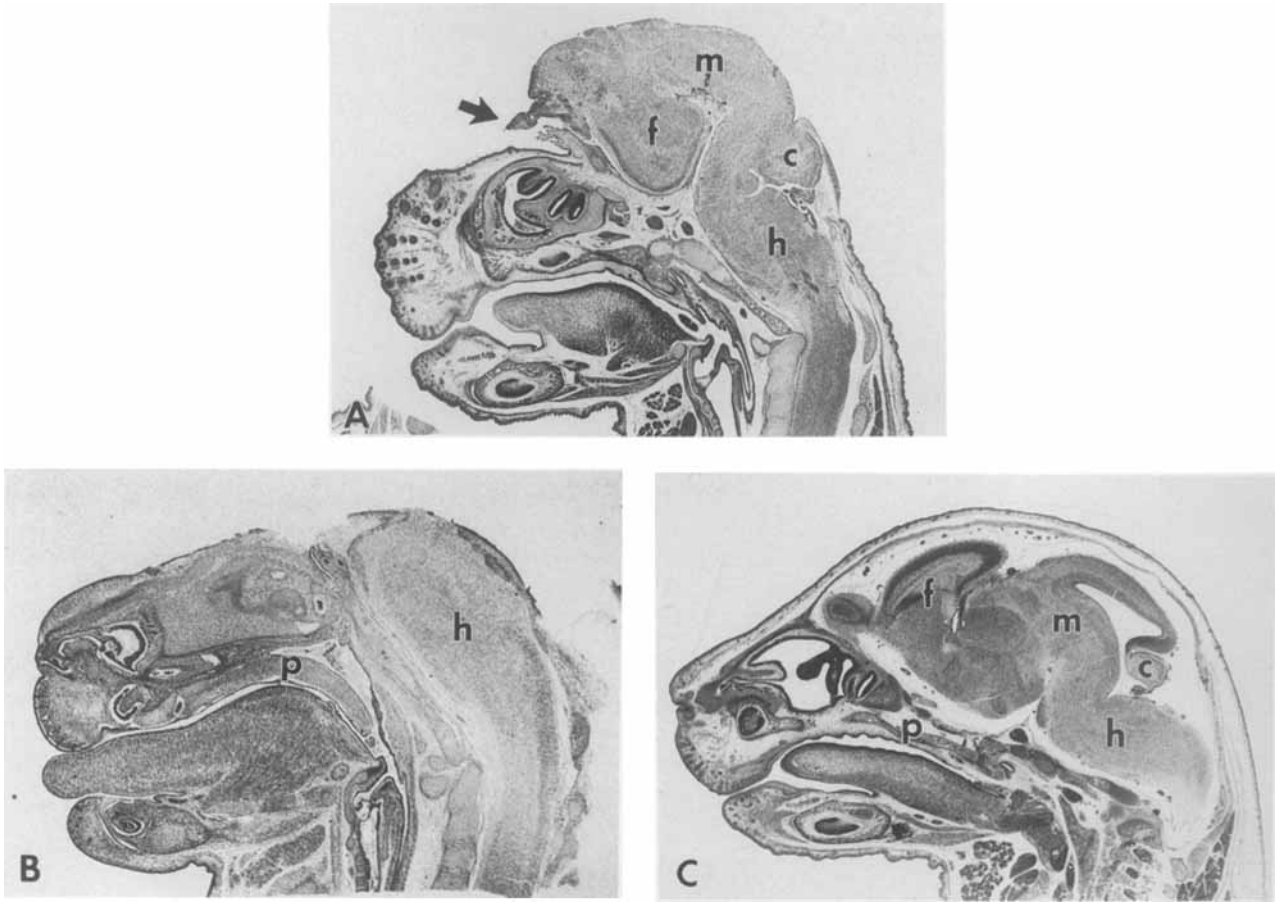

Fig. 5. Parasagittal sections of mouse fetuses (GD 17) with methanol-induced cephalic dysraphism. In fetuses with exencephaly (**A**), the everted midbrain (m) often extended forward over the forebrain (f), which is rotated laterally and caudally. Necrosis and hemorrhage in exposed neural tissue was variable but extensive. In contrast, the hindbrain (h) is the only remnant in anencephaly (**B**). The exposed brain surfaces are covered with ependymal cells and choroid plexus (arrow, **A**). Palates (p) were elevated in many dysraphic fetuses, and some also had dysplastic teeth (**B**). **C:** Control. c, cerebellum. Hematoxylin & eosin, ×7.5.

ventricle and a narrow, elongated facial conformation (H, Fig. 4). Microcephaly, indicated by a visible reduction in head size relative to that of the body, was a consistent finding in fetuses with dysraphic defects but was also grossly evident in some methanol-exposed fetuses that were otherwise overtly normal.

Histopathologic evaluation of malformed fetuses revealed a plethora of qualitative lesions. Relative to controls, the cerebral cortices of exencephalic fetuses were displaced caudally, ventrally, and laterally, while the basal ganglia, thalamus, and midbrain were displaced both dorsally and cranially (Figs. 5A, 6A, 7A). The brain architecture was approximately symmetrical. The dorsal surface (representing the opened third ventricle) usually consisted of necrotic and hemorrhagic parenchyma lined intermittently by ependymal cells and tufts of choroid plexus. These structures were continuous with the epidermis over the front and sides of the head (Figs. 5A, 6A, 7A). The extent of parenchymal hemorrhage and necrosis was increased markedly in fetuses with severe exencephaly, or anencephaly (Fig. 5B). Focal heterotopias of cortical neurons were present in several exencephalic brains. In fetuses with encephalocele, the brain was covered externally by skin and/or highly vascular meninges, but not by bone. The orientation and thickness of layers in the cerebral cortex were variable immediately beneath the protrusion but were apparently normal at more distant sites. Holoprosencephalic brains consisted of a single, cystic ventricle containing projections of disorganized neural tissue and choroid plexus. The ventricle was lined by a discontinuous layer of cerebral cortex and/or ependyma.

As demonstrated by measurements of cerebral cortical thickness, structural defects also occurred in overtly normal, methanol-exposed fetuses (Table 2). Relative to control brains, the thickness of the frontal cortex was significantly decreased by 7.5% in methanol-exposed fetuses (Fig. 8). This narrowing was associated with significant reductions (at least 17%) in the

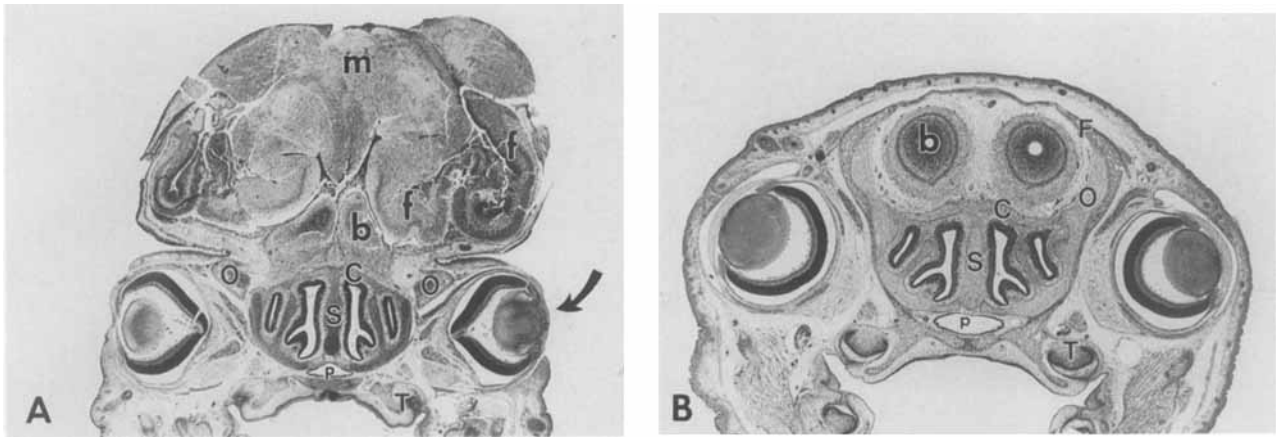

Fig. 6. A: Cross section of the caudal nose (Fig. 1, plane 3) in mouse fetus (GD 17) with methanol-induced exencephaly. Absence of the frontal bone (F) and truncation of the orbitosphenoids (O) have allowed the extruded brain to project forward over the nose. Note the regional reductions of the cribriform plate (C) and nasal septum (S), and the shallow orbital fossae containing conical eyes. The eyelids are abnormally open (arrow). The nasopharyngeal meatus (p) is triangular. f, forebrain; m, midbrain; b, olfactory bulb; T, abnormal molar teeth. **(B):** Control. Hematoxylin & eosin, ×15.

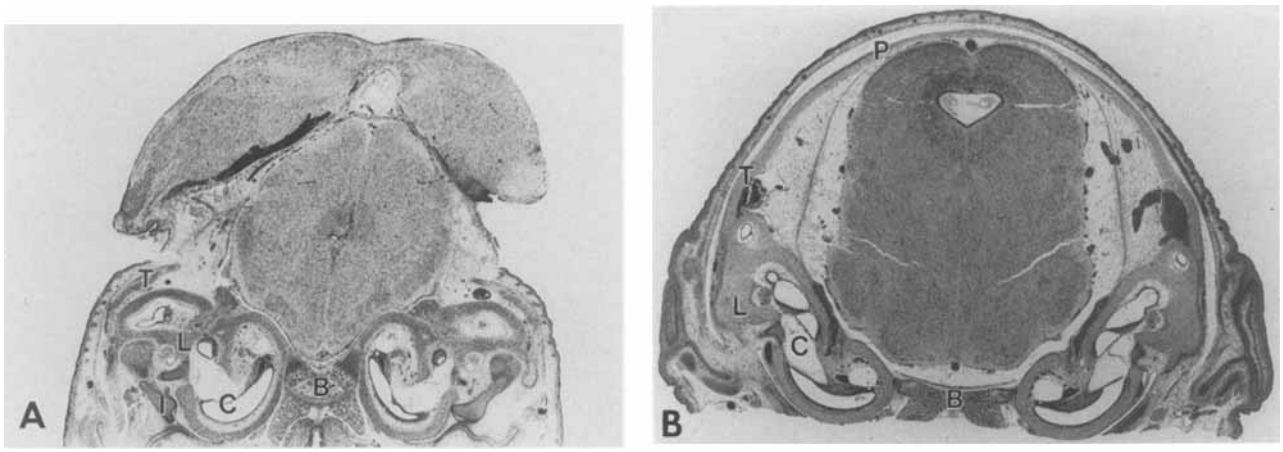

Fig. 7. A: Cross section of the midbrain (Fig. 1, plane 5) in a mouse fetus (GD 17) with methanol-induced exencephaly. The parietal bones (P) are absent bilaterally, and the squamous part of the temporal bones (T) is truncated and rotated inward. The basioccipital (B) is narrow. The petrous temporal bone is deformed, resulting in fewer turns in the osseous labyrinth (L) and cochlea (C). The incus (an otic ossicle; I) is also malformed. **B:** Control. Hematoxylin & eosin, ×15.

thickness of the intermediate cortex/subventricular zone and cortical layer 1, as well as a significant increase of 8.5% in the thickness of the cortical neuropethelium. Qualitatively, the cell density of the subventricular plate in the frontal cortex was also increased (Fig. 8).

Skeletal malformations. A variety of bilaterally symmetrical lesions were noted in the axial skeletons of dysraphic fetuses. Consistent changes included absence of the calvaria (e.g., frontal, parietal, interparietal, and supraoccipital bones), rounding of the basioccipital bone, a reduction (up to 50%) in the length and width of the cranial vault floor, and decreased ossification of bony elements throughout the craniofacial region (Fig. 9). The basisphenoid, orbitosphenoid, maxilla, mandible, ethmoids, and nasal bones were also truncated in at least 40% of affected fetuses (Fig. 9). As a result, gross malformations that often accompanied exencephaly included maxillary and/or mandibular brachygnathism (Fig. 5A,B), elevation or clefting of the palate (Fig. 5B), reduced depth of the orbital fossae, and triangular distortion of the transverse profile of the naso- and oropharynges (Fig. 6A). Remnants of most bones (especially the nasal and orbitosphenoid elements) were rotated laterally (Fig. 6A). However, the squamous portions of the temporal bones were di-

TABLE 2. Thickness of frontal cortex layers in brains of grossly normal fetal mice following maternal inhalation of methanol during neurulation[1]

	Control	Methanol-exposed fetuses[2]	
		All litters	Litters without dysraphism
No. litters	24	16[3]	6
No. fetuses[4]	56	39	14
Neuroepithelium	98.5 ± 1.3	108.8 ± 2.1*	107.1 ± 2.5*
Intermediate cortex and subventricular plate	229.8 ± 3.3	190.9 ± 3.7*	193.6 ± 3.1*
Cortical plate	129.6 ± 1.4	127.3 ± 2.3	128.2 ± 4.0
Cortical layer 1	30.2 ± 0.6	22.9 ± 0.6*	23.4 ± 1.2*
Total thickness, frontal cortex	488.1 ± 3.9	449.9 ± 5.7*	452.3 ± 7.4*

[1]Values are mean ± SE (μm).
[2]Exposure to 15,000 ppm for 6 hr/day during GD 7–9.
[3]Analysis excludes 3 litters in which all fetuses were resorbed and 1 litter in which autolyzed fetuses were not processed for histopathology.
[4]Fetuses (n = 2 or more litter) were chosen at random.
*$P \leq 0.05$, significant difference from age-matched controls by ANOVA and Scheffe's F-test.

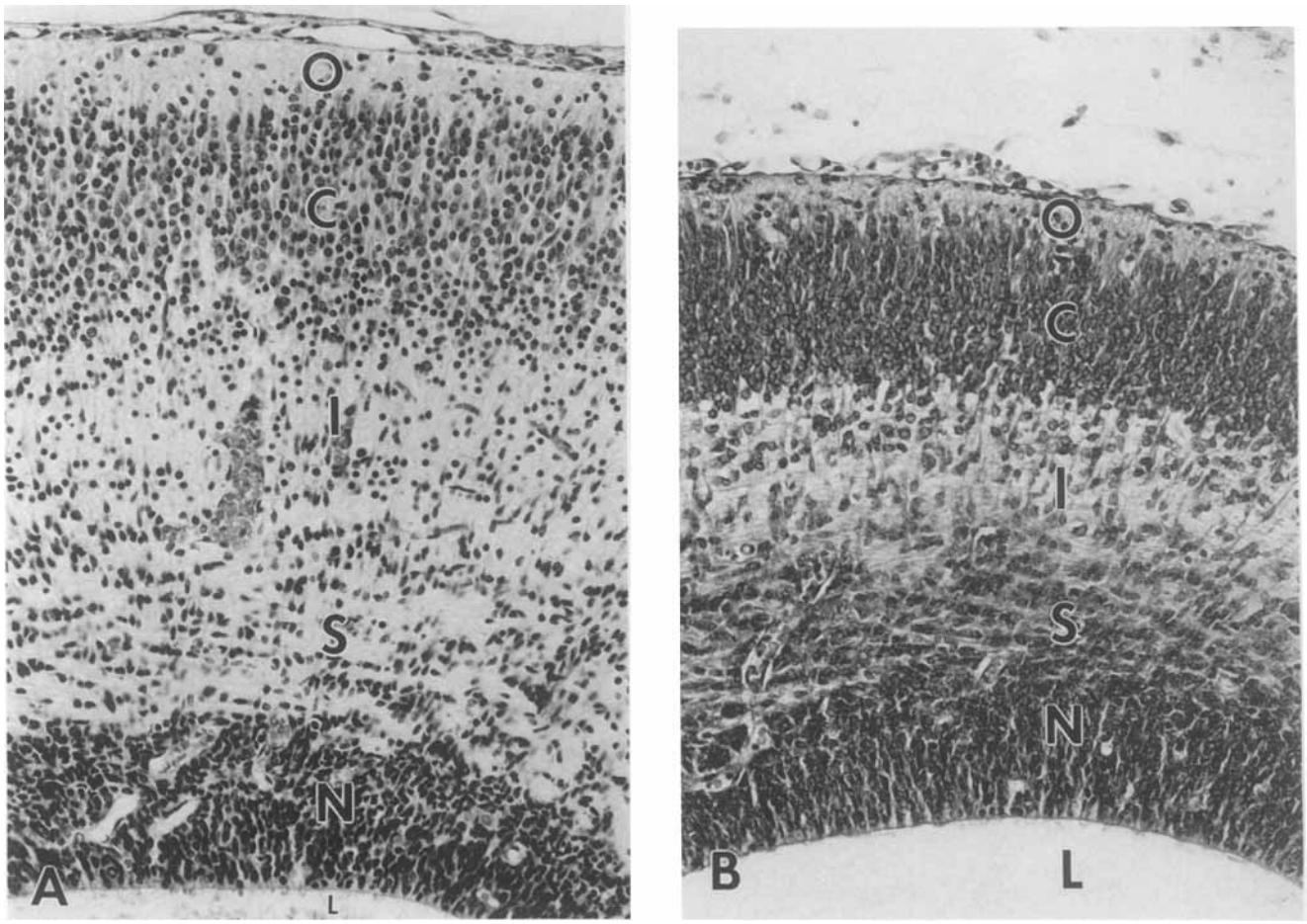

Fig. 8. Transverse sections through the forebrain of GD 17 control **(A)** and methanol-exposed **(B)** mouse fetuses (detail of labeled cortical layers in Fig. 2). Note the decreased thickness of the cerebral cortex, increased thickness of the cortical neuroepithelium (N), and increased cellularity of the subventricular plate (S) and intermediate zone (I). C, cortical plate; O, cortical layer 1; L, lateral ventricle. Hematoxylin & eosin, ×200.

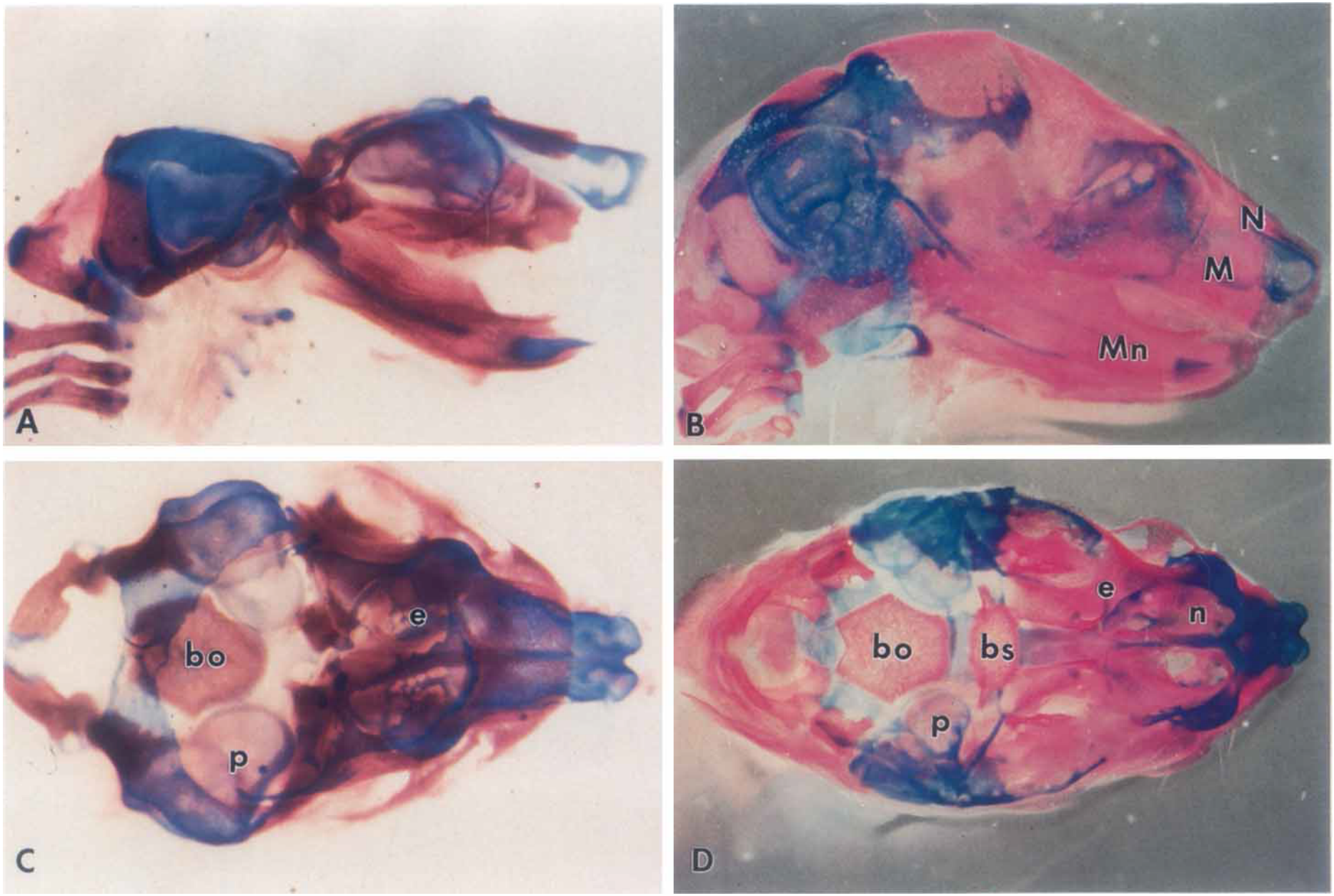

Fig. 9. A,C: Double-stained, cleared heads of exencephalic fetal mice (GD 17) showing absence of the calvaria; reduction of the basisphenoid (bs), basioccipital (bo), ethmoid (e), maxilla (M), mandible (Mn), and nasal (N,n) bones; and decreased ossification (light red) in methanol-induced dysraphism. **B,D:** Control. p, osseous labyrinth of petrous tempral bone. Alcian blue and alizarin red S, ×12.

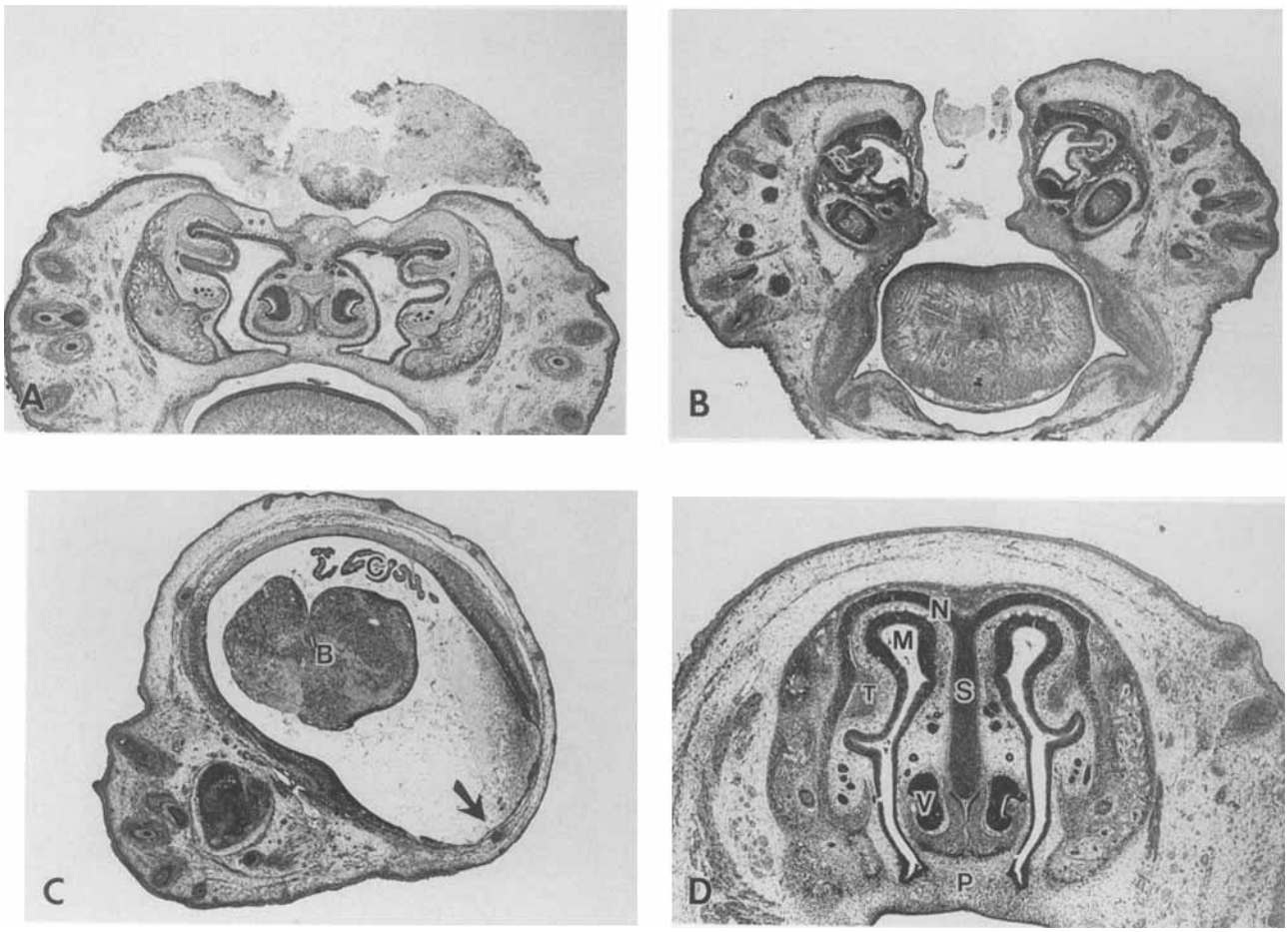

Fig. 10. Cross sections of the rostral nose (Fig. 1, plane 1) in mouse fetuses (GD 17) with methanol-induced exencephaly. The skin, connective tissue, and nasal capsule (N) covering the dorsal surface are incompletely fused, and the dorsal medial meati (M) and nasoturbinates (T) are rotated to the side in moderate cases **(A)**. In more severe cases **(B)**, the entire nose is cleft to the oral cavity. In some holoprosencephalic fetuses **(C)**, the facial skeleton was absent, and the single cerebral ventricle that extended into the snout was lined by abnormal cerebral cortex (B) and ependymal cells (arrow). **D:** Control. S, nasal septum; V, vomeronasal organ; P, palate; C, choroid plexus. Hematoxylin & eosin, ×16.

rected medially beneath the extruded neural tissue (Fig. 7A). The osseous labyrinths of the petrous temporal bones had fewer turns (Fig. 7A). The otic ossicles were malformed. The incisor and molar teeth of a few fetuses were dysplastic (Figs. 5B, 6B), and in one holoprosencephalic specimen the entire facial skeleton was absent (Fig. 10C).

Several other skeletal defects were observed in exencephalic fetuses with midline snout clefts. The severity of these anomalies depended upon the depth of the rift. Clefting ranged from mild (extending through the cartilaginous capsule) to severe (affecting both the nasal cavity and palate). The most prominent changes were distortion of the nasal capsule and reduction of the septal cartilage (Fig. 10). Lateral rotation of the nasal bones resulted in reduction of the nasoturbinates and attenuation of the dorsal medial nasal meatus. The ventral aspect of the vomeronasal organs was sometimes rotated laterally.

Examination of cleared fetuses that had been exposed as embryos to methanol revealed disruption of segmental differentiation in extracranial regions of the axial skeleton. Relative to controls, the shape, symmetry, and degree of ossification were altered in the cervical vertebrae of several fetuses. In 2/8, the atlas was duplicated, and the rostral cervical vertebrae were partially fused. A transitional vertebra (e.g., the presence of supernumerary ribs on cervical vertebra 7) was present in 8/8 methanol-exposed fetuses, but was absent in all controls.

Ocular anomalies. Premature opening of one or both eyelids with mild to severe exophthalmos occurred in 44% of exencephalic fetuses (Bolon et al., '93). Lesions were often bilateral and approximately symmetrical. Relative to the round shape of closed eyes in controls, cross-sectional profiles of the open eyes observed in exencephalic fetuses were generally conical (Figs. 6A, 11A). The exposed corneal stroma was vacuolated,

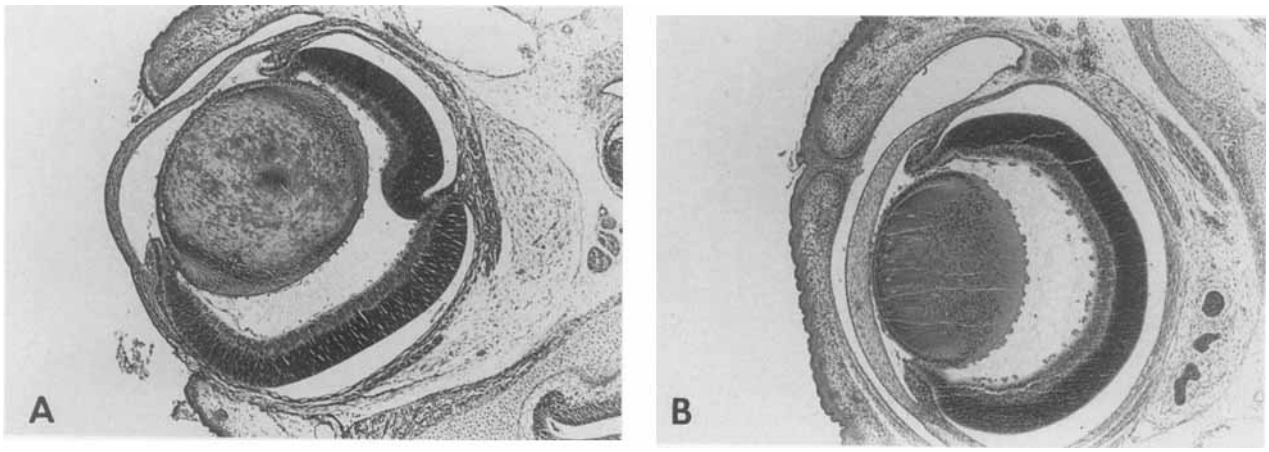

Fig. 11. A: Methanol-induced ocular anomalies in an exencephalic mouse fetus (GD 17). Note the conical profile, wide palpebral fissure, cataract, and retinal fold. **B:** Control. Hematoxylin & eosin, ×150.

and its surface epithelium was often attenuated or absent. Cataracts in the lens stroma consisted of vacuolated and pale fibers with degeneration of the posterior lens epithelium (Fig. 11A). In addition, unilateral retinal folds (Fig. 11A) were observed in a few methanol-exposed fetuses, but not in controls.

Soft tissue defects. Many fetuses with neural tube defects had hypoplastic tongues and aural pinnae. In addition, the skin and connective tissue over the midline of the dorsal snout and forehead were incompletely closed in fetuses with dysraphic defects (Fig. 10). In these regions, follicles of vibrissae and other hairs were reduced both in size and number, and the subcutis was rarefied.

Embryo pathology

Normal anatomy. The timing of major events in primary neurulation (i.e., neural fold formation, elevation, and fusion) in control CD-1 mouse embryos was similar to that described for other mouse strains (Jacobson and Tam, '82; Sakai, '89; Kaufman, '92). Differences in the developmental stage of embryos were apparent both within and between litters by comparison of somite counts and other anatomic features. Briefly, fusion between apposing neural folds was initiated at the junction of the rhombencephalon and spinal cord by GD 8.5. Additional sites of fusion formed subsequently at the apex of the prosencephalon and then at the junction of the prosencephalon and mesencephalon. Neural tube closure proceeded both cranially and caudally from these sites; the mesencephalon fused last, usually at or just after GD 9. As closure proceeded in control embryos, the neural fold margins curled medially in a symmetric fashion (Fig. 12A), yielding a progressively narrower cleft. This gap was finally bridged by a translucent membrane composed of a neuroectodermal sheet covered by coalescing islands of surface ectoderm. By GD 9.5, ingrowth of mesoderm converted the thin membrane into an opaque, multilayered roof (Fig. 13A). After closure, the neurocele had an elliptical cross section.

The pattern of Nile blue sulfate staining in control embryos was similar to that reported for age-matched controls (Sulik et al., '88).

Gross pathology. The anterior neuropore was completely closed by GD 9.5 in almost all (94%) controls but in only 63% of methanol-exposed embryos. Relative to developmental stage-matched controls, treated embryos exhibited delays in growth and rotation and were microcephalic at all times during gestation, regardless of whether the neural tube had closed (Fig. 12B, Table 3). In embryos with cephalic dysraphic defects, the neural tube opening always involved the mesencephalon; the prosencephalon and, to a lesser extent, the cranial rhombencephalon were cleft in only about 10% and 3% of embryos, respectively. The severity and extent of cephalic dysraphism were variable. The neural folds of severely affected embryos were hypoplastic and everted, and the margins in some were notched (Figs. 13B, 14B, 15). In more moderate cases, persistent patency occurred as a narrow (≤0.5 cm) cleft. Relative to the few GD 9 controls with this condition, the unfused neural fold margins of methanol-exposed embryos (at least 10% at GD 9 and 9.5) were rounded, and the boundary between the neuroepithelium and surface ectoderm was abrupt. Mild defects were grossly evident in 13% of methanol-exposed embryos as distortions in mesencephalic conformation (Figs. 13C, 14C). In these occult lesions, the neurocele had collapsed, and the lateral walls and roof of the mesencephalon were translucent and wrinkled due to the reduced quantity of mesoderm; in addition, the neural fold margins were bridged only by bilayered membranes of neuroepithelium and surface ectoderm (Fig. 13C). The heads of many embryos (GD 9 or older) were distorted by the presence of additional lesions, including unilateral or

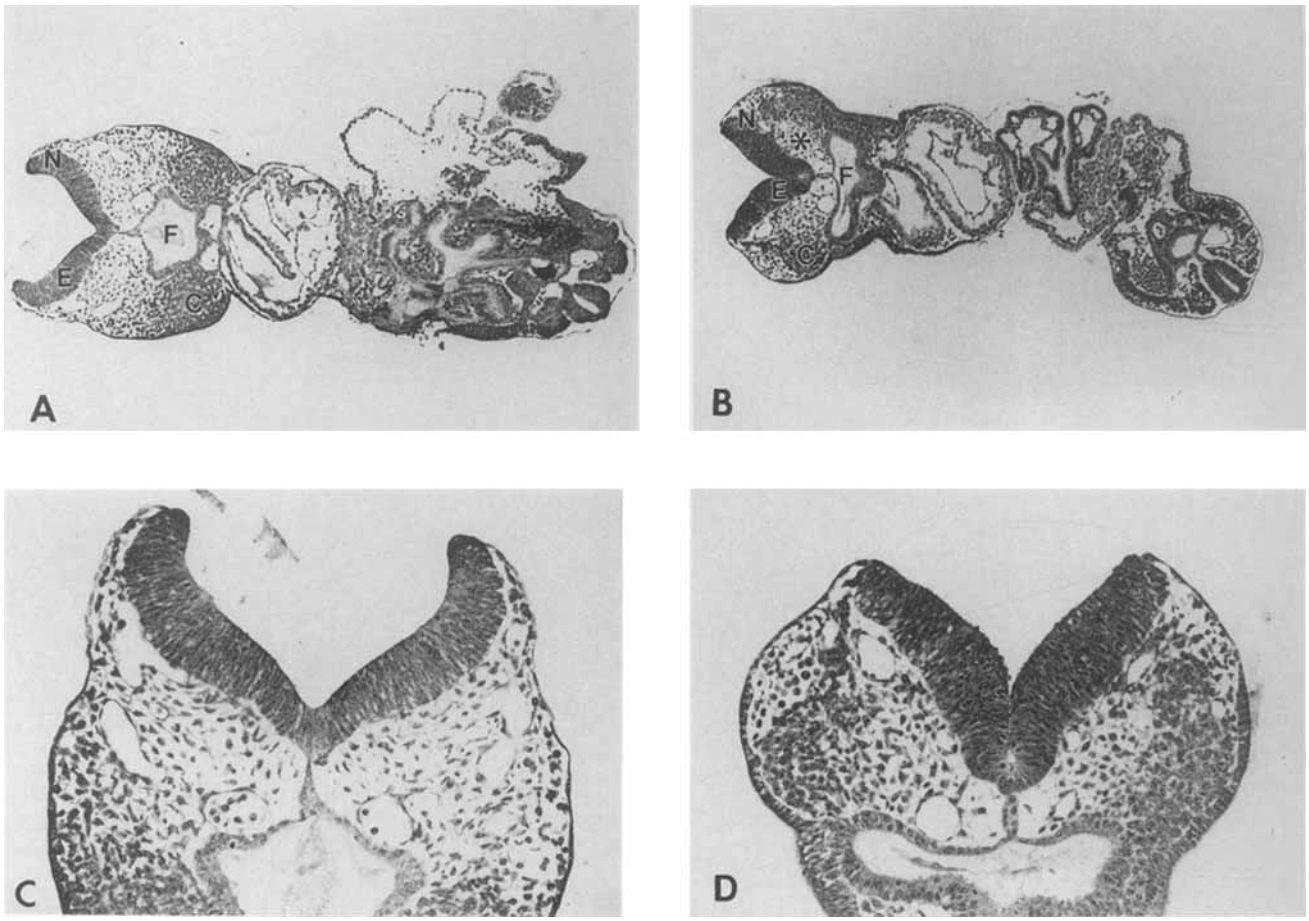

Fig. 12. Longitudinal sections of GD 8.5 mouse embryos showing cephalic pathology induced by maternal inhalation of methanol (15,000 ppm, 6 hr/day) on GD 7–8. When compared to a control embryo **(A,C)**, numerous changes are visible in the microcephalic, methanol-exposed embryo **(B,D)**. Anomalous cephalic structures that were consistently present included hypoplasia and rounding of the neural folds (N), insufficiency (*) of the mesoderm, and collapse of the foregut (F). In some treated embryos, the neuroepithelium **(E)** at the base of the opposing neural folds was in contact, while the neuroectodermal layer at the midline was narrowed. Relative to controls, groups of neural crest cells (C) were often displaced into the neural fold mesoderm cranial to the foregut. Measurements of cell density and mitotic index were obtained bilaterally for the labeled areas of the neuroepithelium and mesoderm from three serial sections of some embryos. Hematoxylin & eosin, ×70 (A,B); ×160 (C,D).

bilateral hypoplasia of the prosencephalon (18% at GD 9 and 95% at GD 10.5) and optic vesicles (18% at GD 9) (Table 4). Additional gross abnormalities that were observed sporadically (≤2.5% incidence) in methanol-exposed embryos included asymmetry of the thalamic adhesions and otic pits (GD 9); distension of one or more primary brain vesicles (GD 9); reduction or absence of branchial arches I and II (GD 9 and 9.5; Fig. 14B); hydropericardium (GD 9.5 or 10.5); scoliosis, with or without multiple reopenings of the thoracic neural tube (GD 9.5); and large vesicles (Fig. 16) located unilaterally at the junction of the prosencephalon and mesencephalon. The origin or contents of these translucent bubbles were not apparent. With the exception of the thalamic changes, the lesions were asymmetric and affected the left side about twice as often. Severe anasarca (generalized edema) was observed in 62% of live embryos at GD 10.5. Finally, maternal methanol exposure resulted in a higher incidence of dead embryos or empty decidua at GD 9, 9.5, and 10.5 (range, 15–38%). Where present, these conceptuses were hemorrhagic and had slowed heart beats and morphologic features characteristic of developmental stages that had occurred in controls about 12–24 hr earlier during

Fig. 13. Cross sections of GD 9.5 mouse mouse embryos showing a continuum of cephalic pathology induced by maternal inhalation of methanol (15,000 ppm, 6 hr/day) on GD 7–9. When compared to a control embryo **(A)**, dysraphism was characterized by persistent patency **(B)** or incomplete fusion **(C)** of the anterior neuropore in association with edema of the mesoderm (M) and distortion of the neurocele (N). Superficial foci of neuroepithelial necrosis (open arrow) with exfoliation of debris into the neurocele were apparent in some embryos with open neuropores **(B)**. The abnormal fusion site (closed arrow) in embryos with occult dysraphism **(C)** was bridged by monolayer sheets from the neuroepithelium and surface ectoderm, but not by mesoderm. O, optic vesicle. Hematoxylin & eosin, ×130.

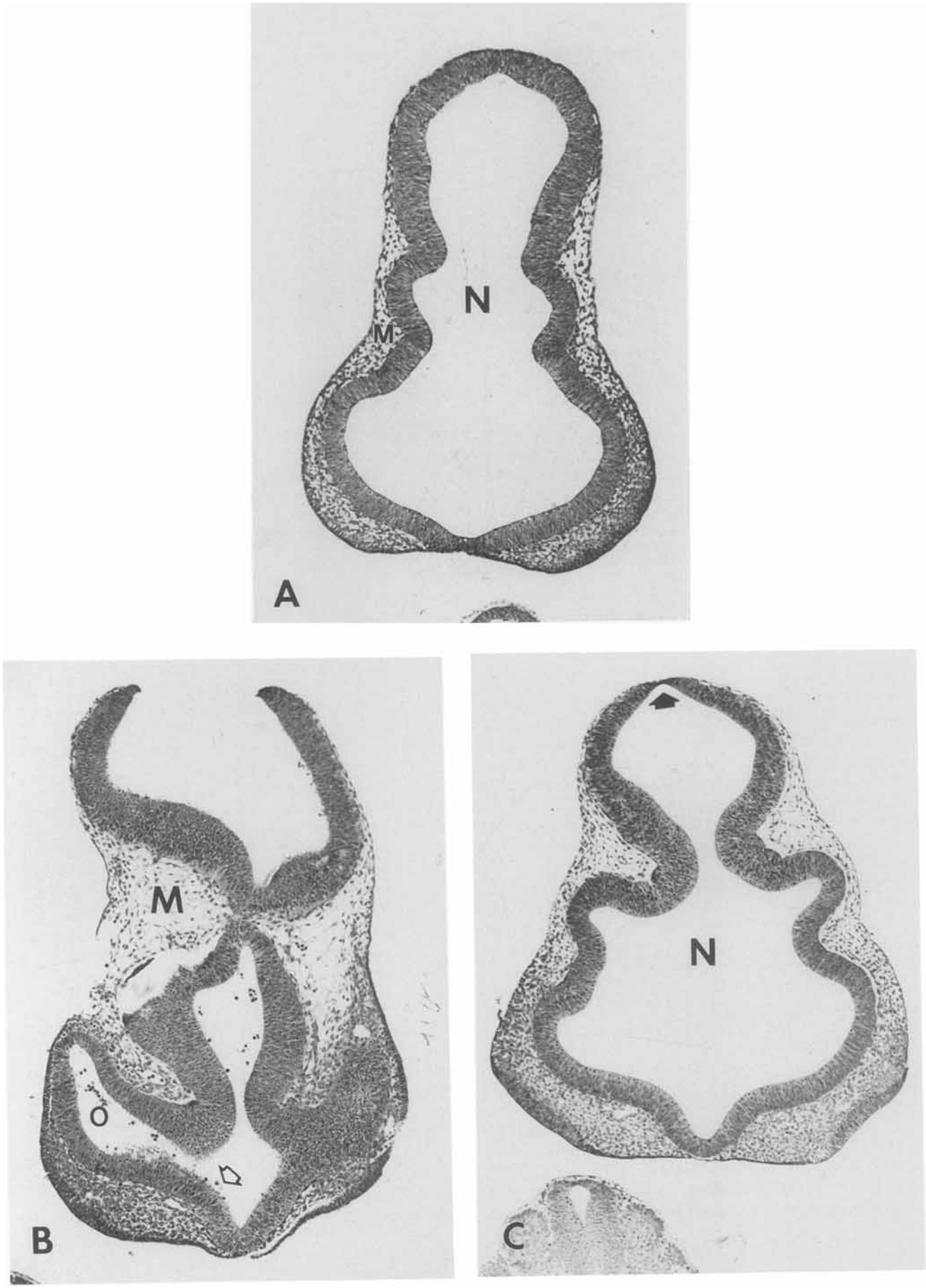

Fig. 13.

TABLE 3. Developmental stage-specific embryotoxicity induced by methanol inhalation during neurulation[1]

No. of somites	Embryonic measurement[3]	Control			Methanol[2]		
		n	Mean (mm)	SD	n	Mean (mm)	SD
16–20	Body length	12	2.43	0.2	28	2.24	0.4
	Head length		1.01	0.1		0.84*	0.3
	FOR length		0.56	0.1		0.49*	0.1
	FOR height		0.50	0.1		0.36*	0.1
21–25	Body length	27	3.15	0.3	94	2.93*	0.5
	Head length		1.45	0.2		1.12*	0.3
	FOR length		0.77	0.1		0.65*	0.2
	FOR height		0.59	0.1		0.54	0.1
26–30	Body length	27	3.76	0.4	33	3.51*	0.5
	Head length		1.82	0.2		1.45*	0.3
	FOR length		0.91	0.1		0.81*	0.2
	FOR height		0.66	0.1		0.62	0.2
31–35	Body length	42	5.21	0.4	20	4.57*	0.5
	Head length		2.67	0.3		2.10*	0.4
	FOR length		1.05	0.1		1.00	0.2
	FOR height		1.01	0.1		0.80*	0.2
36–40	Body length	9	5.41	0.2	14	4.59*	0.5
	Head length		2.77	0.3		2.14*	0.4
	FOR length		1.12	0.1		1.18	0.2
	FOR height		1.03	0.1		0.90	0.3

[1]Measurements compiled from litters on GD 9, 9.5, and 10.5. Embryos were pooled by somite number (i.e., developmental stage) for analysis because of the significant tendency to delayed morphogenesis observed for methanol-exposed embryos.
[2]Exposure to 15,000 ppm for 6 hr/day during GD 7–8 (for GD 9) or 7–9 (for GD 9.5, 10.5).
[3]FOR = forebrain (prosencephalon or telencephalon).
*$P \leq 0.05$, statistically different from control value by ANOVA and Scheffe's tests.

gestation. The incidence of embryonic loss in controls at all time points and in methanol-exposed embryos on GD 8.5 was 8%.

As assessed by Nile blue vital dye staining, the sites and extent of cell death were essentially identical between methanol-exposed embryos and developmental stage-matched controls. Dye was present in scattered neuroectodermal and epithelial cells in all embryos. Significant accumulation occurred only in some of the methanol-exposed conceptuses in tissues around the rim of the otic pit (especially on the right side) and, occasionally, in foci at or adjacent to the neural fold margin (GD 9).

Histopathology. A variety of anomalous cephalic structures were observed in methanol-exposed embryos. A decrease in the amount of mesoderm supporting the cephalic neural folds was the principal microscopic lesion seen in ≥80% of GD 8.5 embryos, most of which were microcephalic (Fig. 12B,D). Additional qualitative findings in <40% of methanol-exposed embryos were 1) the abnormal presence and reduced quantity of neural crest cell columns dorsal to the foregut diverticulum, rather than in the solid sheets that were characteristic of the branchial arches of control embryos (Fig. 12B), 2) narrowing of the neuroepithelium at the base of the neural groove (Figs. 12B, 15, 16), 3) collapse of the foregut (Fig. 12B), and 4) edema of the cranial mesenchyme in older (GD 9.0, 9.5, 10.5) embryos (Figs. 13, 15). Occasional degenerating cells were present in the mesoderm of a few GD 8.5 embryos. The neural folds were apposed at the base of the neural groove on GD 8.5 (Fig. 12), and the analogous regions of the neurocele remained narrow in older embryos with dysraphism (Figs. 13, 15, 16). Relative to controls, blood vessels (particularly on the left side) were sometimes congested and surrounded by hemorrhages (Fig. 16). On GD 9.5 and 10.5, scattered foci of necrosis in the superficial neuroepithelium with exfoliation of debris into the neurocele and optic vesicles were apparent in the heads of a few dysraphic embryos (Fig. 13). Necrosis was particularly prominent on GD 10.5 in the exposed neuroepithelium of the everted neural folds.

Morphometric measurements on GD 8.5 embryos showed that the cell density of paraxial mesoderm was reduced by 47%, and mitotic indices of the mesoderm and neuroepithelium were decreased when compared to control levels to about 17% and 48%, respectively (Table 5).

DISCUSSION

In the present work, a continuum of major gross manifestations including both neural anomalies (e.g., "neural tube defects") and terata of the adjacent skeleton and eyes was observed in dysraphic mouse fetuses that had been exposed to 15,000 ppm of methanol during neurulation. The morphologic appearance and incidence of these lesions were comparable to those reported previously in fetuses of this mouse strain following maternal methanol inhalation (Rogers et al.,

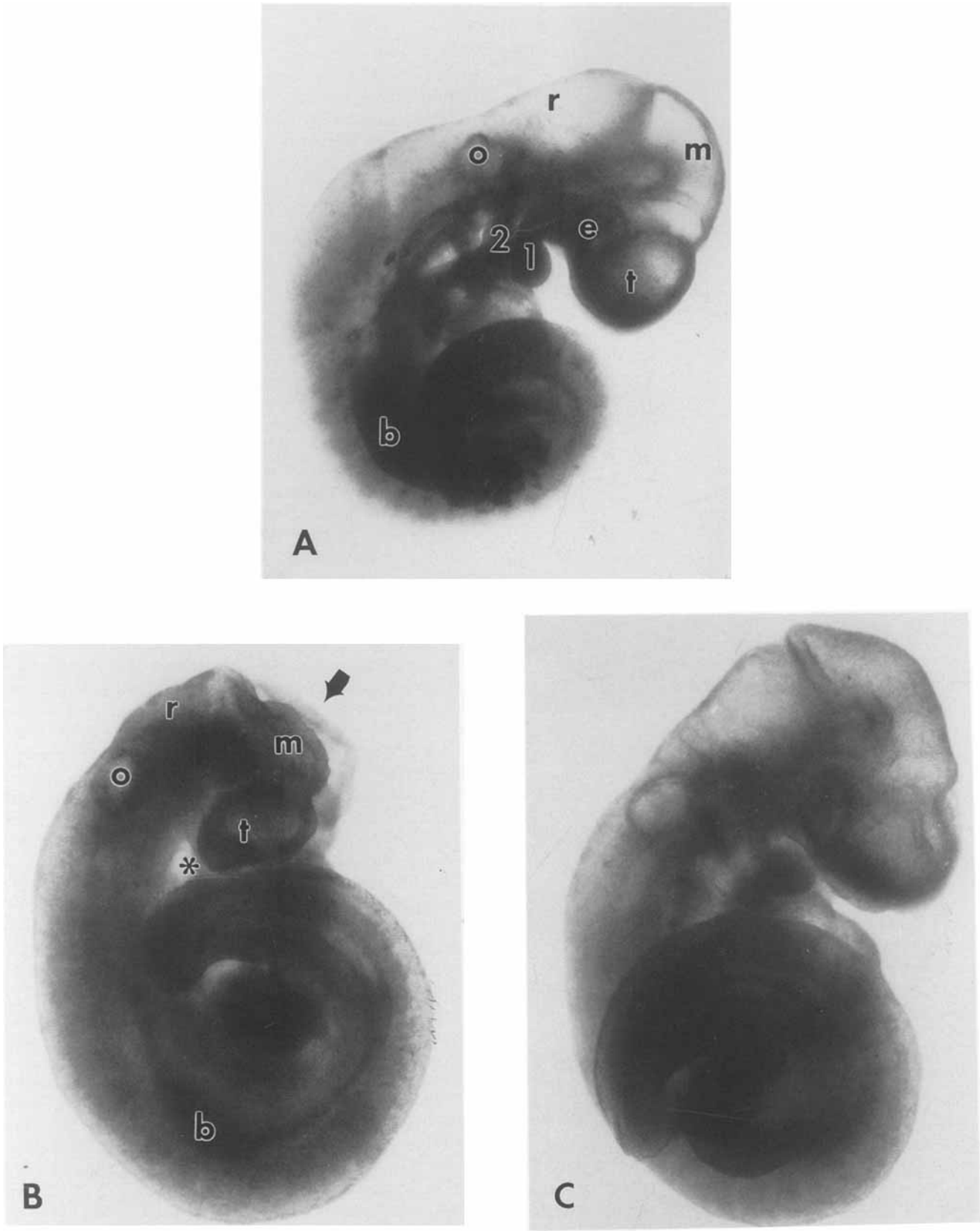

Fig. 14. Profiles of GD 10.5 mouse embryos showing a continuum of cephalic pathology induced by maternal inhalation of methanol (15,000 ppm, 6 hr/day) on GD 7–9. Relative to controls (**A**), overt dysraphism (**B**) was characterized by microcephaly with persistent patency of the mesencephalon (arrow); the unfused neural folds were usually everted. **C:** Occult dysraphism was associated with narrowing and angularity of the mesencephalon. Hypoplasia of the eye and the branchial arches (*) were prominent ancillary lesions (**B**). t, telencephalon; m, mesencephalon; r, rhombencephalon; e, optic vesicle; o, otic pit; b, forelimb bud; 1 and 2, first and second branchial arches. ×45.

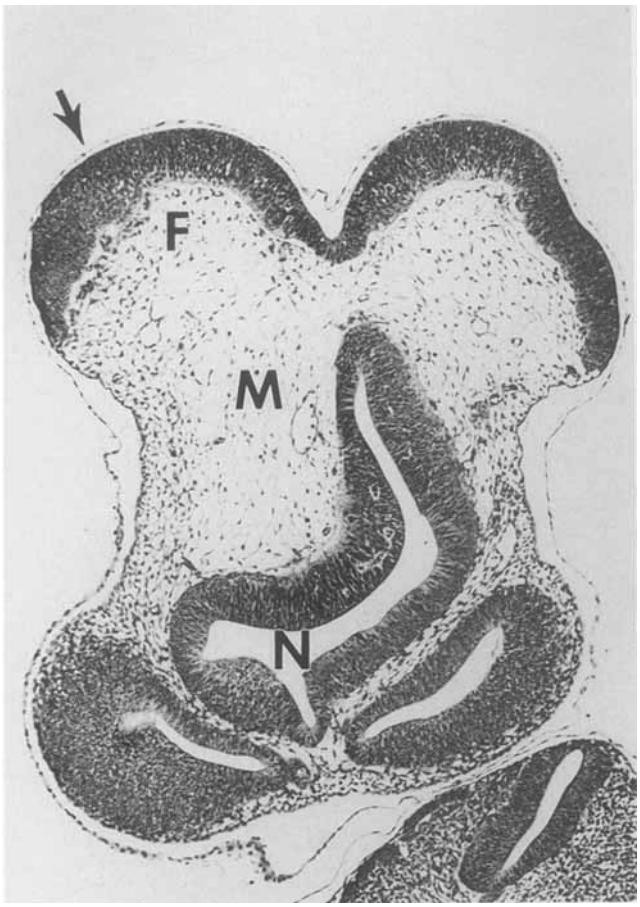

Fig. 15. Cephalic cross section of a GD 10.5 dysraphic mouse embryo following maternal inhalation of methanol (15,000 ppm, 6 hr/day) on GD 7–9. Persistent patency of the mesencephalon was associated with abnormal configuration of the neurocele (N) and edema of the mesoderm (M). In embryos with severe dysraphism, the neural folds (F) were everted, and the exposed neuroepithelium was degenerating (arrow). Hematoxylin & eosin, ×100.

'93). Using this same exposure paradigm, a variety of lesions was produced in neurulating embryos, including the consistent induction of severe cephalic dysraphism and hypoplasia of the prosencephalon, optic vesicles, and branchial arches. This spectrum of methanol-induced damage in embryos correlated well with the types, location, and severity of terata in fetuses, suggesting that the early lesions were involved in the pathogenesis.

The present observations have advanced our understanding of the mechanisms by which methanol induces dysraphic defects. Preceding studies revealed that these malformations result from defective closure of the neural tube (Bolon et al., '93). The current data indicated that this failure appears to be attributable to an inability to raise the neural folds, resulting in persistent patency of the anterior neuropore. Tissues that border this opening (neuroepithelium, neural crest cells, mesoderm) represent likely targets for toxicants (for review, see Campbell et al., '86). The present work indicated that methanol-induced damage to all three of these domains may be involved in this disruption.

A major role for mesodermal injury in embryos as a prelude to dysraphic defects is suggested by the universal presence of terata in structures derived from this tissue. In fetuses with neural tube defects, bones in the calvaria (neurocranium) and basicranium were consistently and severely distorted. These skeletal elements, which are commonly the most disturbed axial segments in dysraphic embryos (Marin-Padilla, '65, '79), are almost entirely derived from paraxial mesoderm (McClone and Bondareff, '75; Jones et al., '82; Noden, '86; Marin-Padilla, '91; Müller and O'Rahilly, '91). Damage to the cephalic mesoderm is commonly detected prior to changes in other tissues of dysraphic embryos (Marin-Padilla, '65; Marin-Padilla and Ferm, '65; Morriss-Kay and Putz, '86; Carpenter, '87; Müller and O'Rahilly, '91). Defective formation and migration of mesoderm have been demonstrated in neurulating embryos following exposure to ethanol (Nakatsuji and Johnson, '84; Sanders et al., '87).

In the present work, mesodermal insufficiency appeared to play a role in the pathogenesis of methanol-induced neural tube defects. This inference may be drawn based on the consistent and severe reductions in the quantity, cell density, and mitotic index of the cranial mesoderm, all of which were seen in methanol-exposed embryos at GD 8.5, 9.0, 9.5, and 10.5. Such alterations would be detrimental to the embryo because the normal development of this tissue is believed to be necessary for control of induction and differentiation of the neuroepithelium (for reviews see Saxén, '80; Jessell and Melton, '92) and for driving neural fold elevation. In addition, mesodermal cells provide internal support for the folds (Marin-Padilla, '91) and serve as a possible locus for generating extrinsic forces needed for complete elevation (Gordon, '85). The mechanisms responsible for the reduction of mesodermal cell density were not apparent. One possibility was that methanol killed large numbers of stem cells. Mesenchymal insufficiency is a common finding in poorly elevated neural folds (Marin-Padilla, '66; Morriss, '72; Morriss and Steele, '74; Carpenter, '87) and seems to be associated with selective deterioration of the mesoderm (Marin-Padilla and Ferm, '65; Waterman, '79). In the present work, the presence of rare degenerate cells in the cranial mesoderm of a few methanol-exposed embryos on GD 8.5 suggested that damage to at least a few of these cells might have been lethal. The true extent of the initial cell loss, if any, could have been masked by the capacity for compensatory growth and repair that characterizes embryonic tissues (Waterman, '79; Shum and Sadler, '88; Francis et al., '90). However, because the regenerative process is not fully manifested until hours after chemical exposure has ended, the absence of necrotic debris and/or phagocytes

TABLE 4. Dysmorphogenic effects induced in neurulating mouse embryos by maternal methanol inhalation (15,000 ppm for 6 hr/day)

	Control	Methanol	Control	Methanol	Control	Methanol	Control	Methanol
Gestational days of exposure	7–8	7–8	7–8	7–8	7–9	7–9	7–9	7–9
Gestational day of analysis	8.5	8.5	9.0	9.0	9.5	9.5	10.5	10.5
No. of litters	5	5	3	4	4	9	4	5
Maternal weight[1] (g)	30.4 ± 2.5	30.2 ± 0.5	32.5 ± 0.2	34.3 ± 0.5	32.3 ± 1.5	29.9 ± 0.7	35.1 ± 1.3	36.4 ± 1.2
No. of embryos								
Total	70	63	29	55	54	117	56	68
Total number of implants/litter[1]	14.0 ± 1.5	12.6 ± 0.8	9.3 ± 4.2	13.8 ± 0.5	13.5 ± 0.6	13.0 ± 0.5	14.0 ± 0.4	13.6 ± 0.7
Live	64	58	26	40	50	99	52	42*
No. (%) of live embryos/litter[1]	12.6 ± 1.2 (91)	11.8 ± 0.7 (92)	8.7 ± 4.5 (90)	8.25 ± 1.9 (73)	12.5 ± 0.6 (93)	10.8 ± 0.9 (85)	13.0 ± 0.7 (93)	11.2 ± 1.2 (62)
No. (%) of abnormal live[2]	0	11 (19)	0	34* (85)	0	41* (41)	0	40* (95)
Dysraphism								
Severe	0	6[3]	0	12[3]	0	28	0	13
Moderate	0	0	0	5	0	11	0	6
Occult	0	0	0	0	0	2	0	9
Total	0	6	0	17*	0	41*	0	28*
Prosencephalic hypoplasia								
Unilateral	0	3	0	7*	0	15*	0	11
Bilateral	0	0	0	0	0	0	0	27*
Branchial arch hypoplasia	0	0	0	11*	0	9	0	3
Hydropericardium	0	0	0	1	1	14*	0	9*
Anasarca	0	0	0	0	0	0	0	26*

[1]Values are mean ± SE.
[2]Calculated as the number of abnormal live embryos over the total number of live embryos.
[3]Neural anomalies include swelling and poor elevation of the neural folds.
*$P \leq 0.05$, significant difference from age-matched controls by Mann-Whitney U-test.

within the mesoderm of methanol-exposed embryos suggested that cell death was minimal. Alternatively, injury to mesodermal cells could have been sublethal, serving to prevent cellular functions not related to survival (Lee and Nagale, '85; Francis et al., '90). For example, the mesenchymal cell population normally doubles every 4–5 hr in gastrulating embryos (Snow, '77). This rate is slowed following exposure to ethanol (Pennington et al., '83). The lower level of cell proliferation demonstrated in methanol-exposed embryos also provided support for this conjecture. The mechanisms by which methanol may influence cell proliferation are not known. Finally, edema of the neural folds was considered an explanation for the reductions in mesodermal cell counts. Fluid accumulation would expand the intercellular space and thus decrease the number of cells in a given area. While this phenomenon occurred, edema was rejected as the sole factor responsible for the mesodermal deficit because mild to severe microcephaly and a qualitative reduction in the total area of the mesoderm were always concurrent findings in methanol-exposed embryos.

Methanol-induced craniofacial and ocular terata also reflected damage to neural crest cells. In the head, different domains (from rostral to caudal) of neural crest cells located along the neural fold margins supply precursors for distinct structures of the face (Smits-van Prooijie et al., '85; Müller and O'Rahilly, '91). Because the neural crest does not contribute to the formation of dorsal cephalic structures (Müller and O'Rahilly, '89), lesions in these cells have no direct role in producing the persistent patency of the dorsal cranium and brain. However, these cells migrate through the mesoderm before finally differentiating into elements of the facial skeleton (Nichols, '81; Marin-Padilla, '91), eye (Johnston et al., '79), and other organs. During their migration, neural crest cells provide signals that can program the responses of adjacent mesenchymal cells (Noden, '86). Thus, selective damage to individual groups of neural crest cells could result in a spectrum of facial skeletal defects, a consequence that has been demonstrated previously in mouse conceptuses exposed to ethanol (Sulik and Johnston, '82; Webster et al., '83; Padmanabhan and Muawad, '85; Kotch and Sulik, '92a,b) and which was also apparent in methanol-exposed fetuses in the present study. In addition, histopathologic data gathered in methanol-exposed embryos during the current experiments suggested that defective migration of neural crest cells into craniofacial structures was a possible consequence of maternal exposure to this chemical during neurulation.

The microscopic observations of the present work also suggest that maternal methanol inhalation damages the neuroepithelium. This tissue appears to pro-

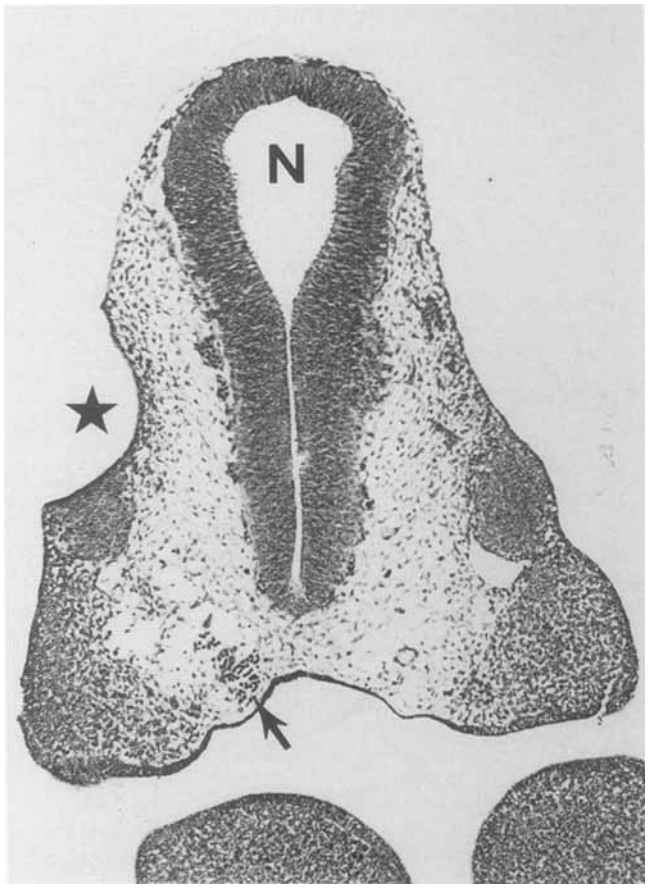

Fig. 16. Cephalic cross section of a GD 9 mouse embryo following maternal inhalation of methanol (15,000 ppm, 6 hr/day) on GD 7–8. A ruptured vesicle (★) and a congested blood vessel surrounded by hemorrhage (arrow) are apparent on the left side of the prosencephalon. The neurocele (N) is narrow. Hematoxylin & eosin, ×65.

vide much of the impetus for elevation of the neural folds (for reviews see Karfunkel, '74), particularly through its intrinsic ability to expand by rapid cell proliferation (Jelínek and Friebová, '66). Decreased neuroepithelial cell division has been postulated as the cause of neural tube defects (Cole and Trasler, '80; Seller, '83). In the present study, neuroepithelial proliferation was reduced concurrently with the mesodermal lesions in some of the GD 8.5 embryos that had been exposed to methanol, raising the possibility that lesions in this tissue may contribute to the induction of neural tube defects. Further detailed time-course experiments will be required to resolve this issue. Important features of the current work were the absence of degenerating cells and vital dye accumulation in the neuroepithelium of methanol-exposed embryos. It appears, therefore, that excessive neuroepithelial cell death was not essential to the pathogenesis of methanol-induced neural tube defects. This characteristic pattern of changes differs from that reported for ethanol, in which an increase in the extent of programmed cell death (apoptosis) in the neuroepithelium of mouse embryos has been described (Sulik et al., '88; Kotch and Sulik, '92a,b). Many factors could have contributed to this discrepancy, including differences in mouse strain (C57BL/6J for ethanol), route (i.p.), and timing (2 doses 4 hr apart on GD 8) of ethanol exposures, or the level and rate at which each alcohol accumulated in the embryo. Another possibility is that methanol and ethanol have different mechanisms of embryotoxicity, perhaps due to the distinct chemical natures of their putative toxic metabolites (formate for methanol, Eells, '91; acetaldehyde for ethanol, O'Shea and Kaufman, '79). Future comparative studies of methanol- and ethanol-induced neural tube defects using a standard experimental design will help to clarify these issues.

Differences in the extent of initial involvement at target sites rather than differing pathogeneses may be responsible for the variable expression of chemically induced brain and craniofacial malformations (McCormick, '71; Marin-Padilla and Marin-Padilla, '81). With this in mind, the present work contributes to our understanding of methanol-induced developmental toxicity in two important ways. First, the rare occurrence of encephalocele suggests that less severe dysraphic lesions may be repaired during later development. This inference is supported by the present data indicating a 3-fold higher incidence of neural tube defects in GD 9.5 embryos (41%) than has been reported for GD 17 fetuses (15%; Bolon et al., '93) after maternal exposure to 15,000 ppm of methanol during GD 7–9. This numerical discrepancy might be explained by the capacity for mild and moderate dysraphic defects in embryos to undergo delayed fusion. Such "catch-up" growth and differentiation (Carpenter, '87; Shum and Sadler, '88; Francis et al., '90) are unlikely to occur after exposure to frank cytotoxicants (Sadler et al., '88), suggesting that methanol-induced cephalic dysraphism was not associated with excessive cell death. This finding was further supported by the absence of significant increases in vital dye accumulation of methanol-exposed embryos. Furthermore, the simple, quantitative observations made during the present study revealed significant microscopic changes in brain structure of methanol-exposed fetuses from litters in which neural terata were absent, principally alterations in the thickness of cerebrocortical layers that contain neurons and their precursors. The pathogenesis of these end-stage methanol lesions was not apparent, but similar changes following ethanol exposure during embryogenesis have been associated with abnormal neurogenesis, defective neuron migration, and aberrant arborization of terminal neurites (Pratt and Doshi, '84; Hammer, '86; West and Pierce, '86). Such micromorphologic aberrations in the brain have been reported in association with persistent behavioral abnormalities in animals and children following maternal exposure to ethanol (Streissguth et al., '80). Taken together, these data indicate that the incidence of gross lesions alone as an

TABLE 5. Cell densities in the cranial mesoderm and neuroepithelium of neurulating mouse embryos following maternal methanol inhalation[1]

	No. litters	No. embryos	No. cells/μm^2		No. mitotic cells/μm^2 (% of total cells)	
			Neuroepithelium	Mesoderm	Neuroepithelium	Mesoderm
Control	2	4	23.3 ± 1.9	16.1 ± 0.3	2.3 ± 0.4 (10.0%)	0.6 ± 0.4 (3.8%)
Methanol[2]	4	10	25.0 ± 0.5	8.6 ± 0.5*	1.1 ± 0.2* (4.4%)	0.1 ± 0.1* (1.2%)

[1]Values are mean ± SE as measured on GD 8.5.
[2]Exposure to 15,000 ppm for 6 hr/day during GD 7–8.
*$P \leq 0.05$, significant difference from controls by the Mann-Whitney U-test.

index of developmental toxicity is likely to underestimate the hazards posed by gestational exposure to high levels of methanol. The significance of such lesions, if any, in assessing risk to human conceptuses following prolonged exposure to low levels of methanol is unknown.

Fluid accumulation in embryonic tissues (e.g., neural folds, subcutis) or cavities (e.g., hydropericardium) was another common finding. Histopathologic lesions associated with methanol-induced ocular toxicity in people (Sharpe et al., '82) are consistent with histotoxic edema resulting from hypoxia and decreased ATP levels. Formate is a potent inhibitor of cytochrome c oxidase, the terminal catalyst of the mitochondrial electron transport chain (Nicholls, '75), and of other enzymes involved in oxidative phosphorylation (Nicholls, '76). Binding of formic acid to the heme iron of this enzyme reduces enzyme activity and thus ATP production (Keyhani and Keyhani, '80). The effects of methanol exposure on mitochondrial function in embryos, and specifically the capacity for ATP biosynthesis, was not determined in the present study, so it could not be stated whether or not altered energy metabolism was responsible for the edema. Additional work is needed to investigate the roles, if any, that fluid imbalances and altered energy metabolism play in the induction of terata.

Many lesions in methanol-exposed embryos that were observed microscopically in the present work occurred asymmetrically. For example, hypoplasia of the prosencephalon and optic vesicles, as well as fluid-filled blisters of the dorsal head, occurred mainly on the left side. Interestingly, asymmetric changes have been observed in the cephalic tissues of mouse embryos cultured with the methanol metabolite, formate (Bolon and Welsch, unpublished data). In particular, staining with 3-[4,5-dimethylthiazol-2-yl]-2,5-diphenyltetrazolium bromide (MTT), a substrate for mitochondrial enzymes that generate ATP (Mosmann, '83), was decreased to a notably greater extent on the left side of the head than on the right. Thus, one explanation for the sidedness of methanol-induced lesions could be regional differences in the energy metabolism of embryonic tissues. An alternative explanation could be that asymmetric lesions resulted from regional alterations in blood flow. Dilated blood vessels on the left side of the head were apparent in some embryos with asymmetric lesions (Coelho and Klein, '90). Furthermore, some of these vessels were congested, suggesting the possibility of sluggish blood flow leading to hypoxia. Indeed, differential oxygenation of cephalic tissues in embryos may be a cause of axial asymmetry in rat embryos cultured in the presence of niridazole (Fantel et al., '86, '89). However, the lesions occurred on the right and were associated with extensive necrosis of both the mesoderm and neuroepithelium. Hypoxia during gastrulation leads to deficiencies in segmented (somitic) and unsegmented (somitomeric) mesoderm (Gallera, '51). Additional work is needed to determine whether or not hypoxia contributes to the pathogenesis of methanol-induced lesions and to ascertain why asymmetric defects were observed in neurulating embryos but not near-term fetuses.

The airborne methanol concentrations to which the general public may be exposed have been estimated to range from less than 1 mg/m^3 (0.75 ppm) for drivers in an urban setting up to a maximum of 650 mg/m^3 (500 ppm) for 15 min for individuals who idle malfunctioning cars in enclosed garages (Kavet and Nauss, '90). Thus, in the present study, the test concentration (15,000 ppm) and treatment length (6 hr/day) exceeded those of the predicted worst-case scenario for methanol inhalation by 30-fold and 24-fold, respectively. Nevertheless, the higher sensitivity of primate species (Roe, '82), and especially folate-deficient groups such as pregnant women and their offspring, to the toxic effects of methanol warrants the acquisition of additional data on exposure-response relationships (e.g., elucidation of species differences in methanol dosimetry and tissue responses during pregnancy) to clarify the potential hazards to the human conceptus at levels likely to be encountered in the environment.

ACKNOWLEDGMENTS

The authors thank Paul Ross, Elizabeth Humphrey, and Leroy Parker for animal care; R. Arden James and Kay Roberts for conducting inhalation exposures; Donald Joyner and Mary Morris for technical assistance; and Drs. David Dorman and Ketti White for editorial

review. Dr. Bolon's gratitude is also extended to the members of his doctoral committee, Drs. Doyle G. Graham (co-advisor) of Duke University, Douglas C. Anthony of Harvard University, Barbara Crain of Johns Hopkins University, and Kevin T. Morgan and Frank Welsch (co-advisor) of CIIT.

LITERATURE CITED

Barrow, M.V., and W.J. Taylor (1969) A rapid method for detecting malformations in rat fetuses. J. Morphol., *127*:291–306.

Bolon, B., D.C. Dorman, and F. Welsch (1993) Phase-specific developmental toxicity in mice following maternal methanol inhalation. Fundam. Appl. Toxicol., *21*:508–516.

Brown, N.A. (1990) Routine assessment of morphology and growth: Scoring systems and measurements of size. In: Postimplantation Mammalian Embryos: A Practical Approach. A.J. Copp and D.L. Cockroft, eds. IRL Press, Oxford, pp. 93–108.

Campbell, L.R., D.H. Dayton, and G.S. Sohal (1986) Neural tube defects: A review of human and animal studies on the etiology of neural tube defects. Teratology, *34*:171–187.

Carpenter, S.J. (1987) Developmental analysis of cephalic axial dysraphic disorders in arsenic-treated hamster embryos. Anat. Embryol., *176*:345–365.

Coelho, C.N.D., and N.W. Klein (1990) Methionine and neural tube closure in cultured rat embryos: Morphological and biochemical analyses. Teratology, *42*:437–451.

Cole, W.A., and D.G. Trasler (1980) Gene-teratogen interaction in insulin induced mouse exencephaly. Teratology, *22*:125–139.

Decker, J.R., O.R. Moss, and B.L. Kay (1982) Controlled-delivery vapor generator for animal exposures. Am. Ind. Hyg. Assoc. J., *43*: 400–402.

Eells, J.T. (1991) Methanol-induced visual toxicity in the rat. J. Pharmacol. Exp. Ther., *257*:56–63.

Fantel, A.G., J.C. Greenaway, E. Walker, and M.R. Juchau (1986) The toxicity of niridazole in rat embryos in vitro. Teratology, *33*:105–112.

Fantel, A.G., M.R. Juchau, C.J. Burroughs, and R.E. Person (1989) Studies of mechanisms of niridazole-elicited embryotoxicity. Evidence that oxygen depletion plays a role in dysmorphogenicity. Teratology, *39*:243–251.

Francis, B.M., J.M. Rogers, K.K. Sulik, A.J. Alles, K.E. Elstein, R.M. Zucker, E.J. Massaro, M.B. Rosen, and N. Chernoff (1990) Cyclophosphamide teratogenesis: Evidence for compensatory responses to induced cellular toxicity. Teratology, *42*:473–482.

Gallera, T. (1951) Influence de l'atmosphère artificiellement modifiée sur le développement embryonnaire du poulet. Acta Anat. (Basel), *11*:549–585.

Gordon, R. (1985) A review of the theories of vertebrate neurulation and their relationship to the mechanisms of neural tube birth defects. J. Embryol. Exp. Morphol., *89*:229–225.

Hammer, R.P. (1986) Alcohol effects on developing neuronal structure. In: Alcohol and Brain Development. J.R. West, ed. Oxford University Press, New York, pp. 184–203.

Jacobson, A.G., and P.P.L. Tam (1982) Cephalic neurulation in the mouse embryo analyzed by SEM and morphometry. Anat. Rec., *203*: 375–396.

Jacobson, M. (1992) Developmental Biology, 3rd ed. Plenum Press, New York.

Jelínek, R., and Z. Friebová (1966) Influence of mitotic activity on neurulation movements. Nature, *209*:822–823.

Jessell, T.M., and D.A. Melton (1992) Diffusible factors in vertebrate induction. Cell, *68*:257–270.

Johnston, M.C., D.M. Noden, R.D. Hazelton, J.L. Coulombre, and A.J. Coulombre (1979) Origins of avian ocular and periocular tissues. Exp. Eye Res., *29*:27–43.

Jones, M.C., K.L. Jones, and G.F. Chernoff (1982) Possible mesodermal origin for axial dysraphic disorders. J. Pediatr., *101*:845–849.

Karfunkel, P. (1974) The mechanisms of neural tube formation. Int. Rev. Cytol., *38*:245–271.

Kaufman, M.H. (1992) The Atlas of Mouse Development. Academic Press, San Diego.

Kavet, S., and K.M. Nauss (1990) The toxicity of inhaled methanol vapor. CRC Crit. Rev. Toxicol., *21*:21–50.

Keyhani, J., and E. Keyhani (1980) EPR study of the effect of formate on cytochrome c oxidase. Biochem. Biophys. Res. Commun., *92*:327–333.

Kimmel, C.A., and C. Trammell (1981) A rapid procedure for routine double staining of cartilage and bone in fetal and adult animals. Stain Technol., *56*:271–273.

Kotch, L.E., and K.K. Sulik (1992a) Experimental fetal alcohol syndrome: Proposed pathogenic basis for a variety of associated fetal and brain anomalies. Am. J. Med. Genet., *44*:168–176.

Kotch, L.E., and K.K. Sulik (1992b) Patterns of ethanol-induced cell death in the developing nervous system of mice: Neural fold states through the time of anterior neural tube closure. Int. J. Dev. Neurosci., *10*:273–279.

Lee, H.-Y., and R.G. Nagale (1985) Studies on the mechanisms of neurulation in the chick: Interrelationship of contractile proteins, microfilaments, and the shape of neuroepithelial cells. J. Exp. Zool., *235*:205–215.

Makar, A.B., and T.R. Tephly (1977) Methanol poisoning. VI. Role of folic acid in the production of methanol poisoning in the rat. J. Toxicol. Environ. Health, *2*;1201–1209.

Marin-Padilla, M. (1965) Study of the sphenoid bone in human cranioschisis and craniorhachischisis. Virchows Arch. Pathol. Anat., *339*:245–253.

Marin-Padilla, M. (1966) Mesodermal alterations induced by hypervitaminosis A. J. Embryol. Exp. Morphol., *15*:261–269.

Marin-Padilla, M. (1979) Notochordal-basichondrocranium relationships: Abnormalities in experimental axial skeletal (dysraphic) disorders. J. Embryol. Exp. Morphol. *53*:15–38.

Marin-Padilla, M. (1991) Cephalic axial skeletal-neural dysraphic disorders: Embryology and pathology. Can. J. Neurol. Sci., *18*:153–169.

Marin-Padilla, M., and V. Ferm (1965) Somite necrosis and developmental malformations induced by vitamin A in the golden hamster. J. Embryol. Exp. Morphol., *13*:1–8.

Marin-Padilla, M., and T.M. Marin-Padilla (1981) Morphogenesis of experimentally induced Arnold-Chiari malformation. J. Neurol. Sci., *50*:29–55.

McClone, D.G., and W. Bondareff (1975) Developmental morphology of the subarachnoid space and contiguous structures in the mouse. Am. J. Anat., *142*:295–318.

McCormick, W.F. (1971) Is anencephaly a single entity? A brief note on the morphologic heterogeneity of anencephaly. In: Conference on the Clinical Delineation of Birth Defects, Part VI, Nervous System. D. Bergsma, V. McKusick, C.I. Scott, I.E. Hussels, C. Jackson, and M.W. Lorber, eds. Williams & Wilkins, Baltimore, pp. 94–96.

Morriss, G.M. (1972) Morphogenesis of malformations induced in rat embryos by maternal hypervitaminosis A. J. Anat., *113*:241–250.

Morriss, G.M., and C.E. Steele (1974) The effect of excess vitamin A on the development of rat embryos in culture. J. Embryol. Exp. Morphol., *32*:505–514.

Morriss-Kay, G., and B. Putz (1986) Abnormal neural fold development in mouse trisomy 12 and trisomy 14. II. LM and TEM. Brain Res. Bull., *16*:825–832.

Mosmann, T. (1983) Rapid colorimetric assay for cellular growth and survival: Application to proliferation and cytotoxicity assays. J. Immunol. Methods, *65*:55–63.

Müller, F., and R. O'Rahilly (1989) Mediobasal prosencephalic defects, including holoprosencephaly and cyclopia, in relation to the development of the human forebrain. Am. J. Anat., *185*:391–414.

Müller, F., and R. O'Rahilly (1991) Development of anencephaly and its variants. Am. J. Anat., *190*:193–218.

Nakatsuji, N., and K.E. Johnson (1984) Effects of ethanol on the primitive streak stage mouse embryo. Teratology, *29*:369–375.

Nelson, B.K., W.S. Brightwell, D.R. MacKenzie, A. Khan, J.R. Burg,

W.W. Weigel, and P.T. Goad (1985) Teratologic assessment of methanol and ethanol at high inhalation levels in rats. Fundam. Appl. Toxicol., *5*:727–736.

Nichols, D.H. (1981) Neural crest formation in the head of the mouse embryo as observed using a new histological technique. J. Embryol. Exp. Morphol., *64*:105–120.

Nicholls, P. (1975) Formate as an inhibitor of cytochrome c oxidase. Biochem. Biophys. Res. Commun., *67*:610–616.

Nicholls, P. (1976) The effect of formate on cytochrome aa_3 and on electron transport in the intact respiratory chain. Biochim. Biophys. Acta, *430*:13–29.

Nishimura, H., and K. Shiota (1977) Summary of comparative embryology and teratology. In: Handbook of Teratology. J.G. Wilson and F.C. Fraser, eds. Plenum Press, New York, Vol. 3, pp. 119–154.

Noden, D.N. (1986) Origins and patterning of craniofacial mesenchymal tissues. J. Craniofac. Genet. Dev. Biol. (Suppl.), *2*:15–31.

O'Shea, K.S., and M.H. Kaufman (1979) The teratogenic effect of acetaldehyde: Implications for the study of fetal alcohol syndrome. J. Anat., *128*:65–76.

Padmanabhan, R., and W.M.R.A. Muawad (1985) Exencephaly and axial skeletal dysmorphogenesis induced by acute doses of ethanol in mouse fetuses. Drug Alcohol Depend., *16*:215–227.

Pennington, S.N., J.W. Boyd, G.W. Kalmus, and R.W. Wilson (1983) The molecular mechanism of fetal alcohol syndrome (FAS). I. Ethanol-induced growth suppression. Neurobehav. Toxicol. Teratol., *5*:259–262.

Posner, H.S. (1975) Biohazards of methanol in proposed new uses. J. Toxicol. Environ. Health, *1*:153–171.

Pratt, O.E., and R. Doshi (1984) Range of alcohol-induced damage in the developing nervous system. In: Mechanisms of Alcohol Damage in Utero (Ciba Foundation Symp. 105). Pitman, London, pp. 142–172.

Roe, O. (1982) Species differences in methanol poisoning. Crit. Rev. Toxicol., *10*:275–286.

Rogers, J.M., M.L. Mole, N. Chernoff, B.D. Barbee, C.I. Turner, T.R. Logsdon, and R.J. Kavlock (1993) The developmental toxicity of inhaled methanol in the CD-1 mouse, with quantitative dose-response modeling for estimation of benchmark doses. Teratology, *47*:175–188.

Sadler, T.W., L. Shum, C.W. Warner, and M.K. Smith (1988) The role of pharmacokinetics in determining the response of rodent embryos to teratogens in whole embryo culture. Toxicol. In Vitro, *2*:175–180.

Sakai, Y. (1989) Neurulation in the mouse: Manner and timing of neural tube closure. Anat. Rec., *223*:194–203.

Sanders, E.J., E. Cheung, and E. Mahmud (1987) Ethanol treatment inhibits mesoderm cell spreading in the gastrulating chick embryo. Teratology, *36*:209–216.

Saxén, L. (1980) Neural induction: Past, present, and future. Curr. Top. Dev. Biol., *15*:409–418.

Seller, M.J. (1983) The cause of neural tube defects: Some experiments and a hypothesis. J. Med. Genet., *20*:164–168.

Sharpe, J.A., M. Hostovsky, J.M. Bilbao, and N.B. Rewcastle (1982) Methanol optic neuropathy: A histopathological study. Neurology, *32*:1093–1100.

Shepard, T.H. (1986) Catalog of Teratogenic Agents, 5th ed. Johns Hopkins University Press, Baltimore.

Shum, L., and T.W. Sadler (1988) Embryonic catch-up growth after exposure to the ketone body D,L-beta-hydroxybutyrate in vitro. Teratology, *38*:369–379.

Smits-van Prooije, A.E., C. Vermeij-Keers, R.E. Poelmann, M.M.T. Mentink, and J.A. Dubbeldam (1985) The neural crest in presomite to 40-somite murine embryos. Acta Morphol. Neerl. Scand., *23*:99–114.

Snow, M.H.L. (1977) Gastrulation in the mouse: Growth and regionalisation of the epiblast. J. Embryol. Exp. Morphol., *42*:293–303.

Streissguth, A.P., S. Landesman-Dwyer, J.C. Martin, and D.W. Smith (1980) Teratogenic effects of alcohol in humans and laboratory animals. Science, *209*:353–361.

Sulik, K.K., and M.C. Johnston (1982) Embryonic origin of holoprosencephaly: Interrelationship of the developing brain and face. Scanning Electron Microsc., *1*:309–322.

Sulik, K.K., M.C. Johnston, and M.A. Webb (1981) Fetal alcohol syndrome: Embryogenesis in a mouse model. Science, *214*:936–938.

Sulik, K.K., C.S. Cook, and W.S. Webster (1988) Teratogens and craniofacial malformations: Relationships to cell death. Development, *103(Suppl)*:213–232.

Szabo, K.T. (1989) Congenital Malformations in Laboratory and Farm Animals. Academic Press, New York, pp. 95–143.

Turner, S., M.E. Sucheston, R.M. de Philip, and R.B. Paulson (1990) Teratogenic effects on the neuroepithelium of the CD-1 mouse embryo exposed in utero to sodium valproate. Teratology, *41*:421–442.

U.S. News (1991) Poisoning the border: Many American-owned factories in Mexico are fouling the environment, and their workers aren't prospering. U.S. News & World Report, *110*:32–36.

Waterman, R.E. (1979) Scanning electron microscope studies of central nervous system development. Birth Defects, *15*:55–77.

Webster, W.S., D.A. Walsh, S.E. McEwen, and A.H. Lipson (1983) Some teratogenic properties of ethanol and acetaldehyde in C57BL/6J mice: Implications for the study of the fetal alcohol syndrome. Teratology, *27*:231–243.

West, J.R., and D.R. Pierce (1986) Perinatal alcohol exposure and neuronal damage. In: Alcohol and Brain Development, J.R. West, ed. Oxford University Press, New York, pp. 120–157.